https://doi.org/10.5194/amt-2019-198
Preprint. Discussion started: 29 May 2019

Atmospheric Measurement Techniques
Discussions
Open Access
EGU

Changes in $PM_{2.5}$ Peat Combustion Source Profiles with Atmospheric Aging in an Oxidation Flow Reactor

Judith C. Chow[1,2*], Junji Cao[2,3], L.-W. Antony Chen[4], Xiaoliang Wang[1], Qiyuan Wang[2,3], Jie Tian[2,3], Steven Sai Hang Ho[1,5], Tessa B. Carlson[1], Steven D. Kohl[1], John G. Watson[1,2]

[1]Division of Atmospheric Sciences, Desert Research Institute, Reno, Nevada, USA

[2]Key Laboratory of Aerosol Chemistry and Physics, Institute of Earth Environment, Chinese Academy of Sciences, Xi'an, 710061, China.

[3]CAS Center for Excellence in Quaternary Science and Global Change, Xi'an, 710061, China

[4]Department of Environmental and Occupational Health, University of Nevada, Las Vegas, Nevada, USA

[5]Hong Kong Premium Services and Research Laboratory, Hong Kong, China

[*]Corresponding Author: judith.chow@dri.edu

Abstract

Smoke from laboratory chamber burning of peat fuels from Russia, Siberia, U.S.A. (Alaska and Florida), and Malaysia representing boreal, temperate, subtropical, and tropical regions was sampled before and after passing through a potential aerosol mass-oxidation flow reactor (PAM-OFR) to simulate ~2- and 7-day atmospheric aging. Species abundances in $PM_{2.5}$ between aged and fresh profiles varied by >5 orders of magnitude with two distinguishable clusters: around 0.1% for reactive and ionic species and mostly >10 % for carbon.

Organic carbon (OC) accounted for 58–85 % of $PM_{2.5}$ mass in fresh profiles with low EC abundance (0.67–4.4 %). After a 7-day aging time, degradation was 20–33 % for OC, with apparent reductions (4–12 %) in low temperature OC1 and OC2 (thermally evolved at 140 and 280 °C), implying evaporation of higher vapor pressure semi-volatile organic compounds (SVOCs). Additional losses of OC from 2- to 7-days aging is somewhat offset by the formation of oxygenated organic compounds, as evidenced by the 12–19 % increase in organic mass (OM) to OC ratios. However, the reduction of OM abundances in $PM_{2.5}$ by 3–18 % after 7 days, reconfirms that volatilization is the main loss mechanism of SVOCs. Although the ammonia (NH_3) to $PM_{2.5}$ ratio rapidly diminished with a 2-day aging time, it represents an intermediate profile –not sufficient for completed OC evaporation, levoglucosan degradation, organic acid oxidation, or secondary inorganic aerosol formation.

Week-long aging resulted in an increase to ~7–8 % of NH_4^+ and NO_3^- abundances, but with enhanced degradation of NH_3, low temperature OC, and levoglucosan for Siberia, Alaska, and Everglasdes (FL) peats. Elevated levoglucosan was found for Russian peats, accounting for 35–39 % and 20–25 % of $PM_{2.5}$ mass for fresh and aged profiles, respectively. Abundances of water-soluble organic carbon (WSOC) in $PM_{2.5}$ was >2-fold higher in fresh Russian (37.0 ± 2.7 %) than Malaysian (14.6 ± 0.9 %) peats. While Russian peat OC emissions are largely water-soluble, Malaysian peat emissions are mostly water-insoluble, with WSOC/OC ratios of 0.59–0.71 and 0.18–0.40, respectively.

Source profiles can change with aging during transport from source to receptor. This study shows significant differences between fresh and aged peat combustion profiles among the four biomes that can be used to establish speciated emission inventories for atmospheric modeling and receptor model source apportionment. A sufficient aging time (~one week) is needed to allow gas-

https://doi.org/10.5194/amt-2019-198
Preprint. Discussion started: 29 May 2019

to-particle partitioning of semi-volatilized species, gas-phase oxidation, and particle volatilization to achieve representative source profiles for regional-scale source apportionment.

Keywords: fresh and aged source profiles, atmospheric aging, organic mass, organic carbon, levoglucosan, oxidation flow reactor (OFR)

https://doi.org/10.5194/amt-2019-198
Preprint. Discussion started: 29 May 2019

1 Introduction

Receptor-oriented source-apportionment models have played a major role in establishing the weight of evidence (U.S.EPA, 2007) for pollution control decisions. These models, particularly the different solutions (Watson et al., 2016) to the Chemical Mass Balance (CMB) equations (Hidy and Friedlander, 1971), rely on patterns of chemical abundances in different source types that can be separated from each other when superimposed in ambient samples of volatile organic compounds (VOC) and suspended particulate matter (PM). These patterns, termed "source profiles," have been measured in diluted exhaust emissions and resuspended mineral dusts for a variety of representative emitters. Many of these source profiles are compiled in country-specific source profile data bases (CARB, 2018; Liu et al., 2017; Mo et al., 2016; Pernigotti et al., 2016; U.S.EPA, 2016) and have been widely used for source apportionment and speciated emission inventories.

Chemical profiles measured at the source have been sufficient to identify and quantify nearby, and reasonably fresh, source contributions. These source types include gasoline- and diesel-engine exhaust, biomass burning, cooking, industrial processes, and fugitive dust. Ambient VOC and PM concentrations have been reduced as a result of control measures applied to these sources, and additional reductions have been implemented for toxic materials such as lead, nickel, vanadium, arsenic, diesel particulate matter, and several organic compounds. As these fresh emission contributions in neighborhood- and urban-scale environments (Chow et al., 2002) decrease, regional-scale contributions that may have aged for 2- to 7-days prior to arrival at a receptor gain in importance. These profiles experience augmentation and depletion of chemical abundances owing to photochemical reactions among their gases and particles, as well as interactions upon mixing with other source emissions.

Changes in source profiles have been demonstrated in large smog chambers (Pratap et al., 2019), wherein gas/particle mixtures are illuminated with ultraviolet (UV) light for several hours and their end products are measured. Such chambers are specially constructed and limited to laboratory testing. A more recent method for simulating such aging is the oxidation flow reactor (OFR), based on the early studies of Kang et al. (2007), revised and perfected by several researchers (e.g., Jimenez, 2018; Lambe et al., 2011), and commercially available from Aerodyne (2019a, b). Cao et al. (2019) evaluated the OFR (Aerodyne Research, Inc., Billerica, MA, USA) for potential source emission certification in China, finding that further study and development is

https://doi.org/10.5194/amt-2019-198
Preprint. Discussion started: 29 May 2019

required for this purpose. However, Cao et al. (2019) concluded that the OFR could be suitable for source profile aging experiments in support of regional-scale source apportionment, and this is further investigated in this paper for peat combustion.

Peatland fires produce long-lasting thick smoke that leads to adverse atmospheric, climate, ecological, and health impacts. Smoke from Indonesian and Malaysian peatlands is a major concern in the countries of southeast Asia (Wiggins et al., 2018) and elsewhere where it is transported over long distances. Aged peat smoke profiles are likely to differ from fresh emissions, as well as among the different types of peat in other parts of the world.

Several ground-based, aircraft, shipboard, and laboratory peat combustion experiments have been carried out to better represent global peat fire emissions and estimate their environmental impacts (e.g., Akagi et al., 2011; Iinuma et al., 2007; Nara et al., 2017; Stockwell et al., 2014; 2016). Most peat fire studies report emission factors (EFs) for pyrogenic gases (e.g., methane, carbon monoxide, and carbon dioxide) and fine particle ($PM_{2.5}$, particles with aerodynamic diameter <2.5 microns) mass, with a few studies reporting EFs for organic and elemental carbon (OC and EC) (Hu et al., 2018); no information on $PM_{2.5}$ speciated source profiles including elements, ions, and carbon is available.

Laboratory peat combustion EFs for gaseous carbon and nitrogen species corresponding with the profiles described here, as well as $PM_{2.5}$ mass and major chemical species (e.g., carbon and ions), are reported by Watson et al. (2019). The $PM_{2.5}$ speciated source profiles derive from six peat fuels collected from Odintsovo, Russia; Pskov, Siberia; Northern Alaska and Florida, U.S.A.; and Borneo, Malaysia, representing boreal, temperate, subtropical, and tropical climate regions. Comparisons between fresh (diluted and unaged) and aged (i.e., 2- and 7-days simulated oxidation with an OFR) $PM_{2.5}$ speciated profiles are made to highlight chemical abundance changes with photochemical aging. Objectives are to: 1) evaluate similarities and differences among the peat source profiles from four biomes; 2) examine the extent of gas-to-particle oxidation and volatilization between 2- and 7-days of simulated atmospheric aging; and 3) characterize carbon and nitrogen properties in peat combustion emissions.

2 Experiment

Peat smoke generated in a laboratory combustion chamber was diluted with clean air by factors of three to five to allow for nucleation and condensation at ambient temperatures (Watson et al., 2012). These diluted emissions were then passed through a potential aerosol mass (PAM)-

OFR (Cao et al., 2019; Watson et al., 2019) in the OFR185 mode without ozone (O_3) injection. The OFR UV lamps were operated at 2 and 3.5 volts with a flow rate of 10 L min^{-1}, assuming an average daily hydroxyl (OH) concentration of 1.5 x 10^6 molecules cm^{-3} to translate OH exposures (OH_{exp}) of ~2.6 x 10^{11} and 8.8 x 10^{11} molecules-sec cm^{-3} into ~2- and 7-days of photochemical aging. Cao et al. (2019) summarize published ambient OH measurements that span a range around this assumed daily average, indicating that the real-world aging times can differ by factors of two or more. Nevertheless, the 1.5 x 10^6 molecules-sec cm^{-3} estimate for OH concentration is a *de facto* standard used for OFR aging estimation.

Forty smoldering-dominated peat combustion tests were conducted that included three to six tests for each type of peat fuel. The following analysis uses time-integrated (~40–60 minutes) gaseous and $PM_{2.5}$ filter pack samples collected upstream and downstream of the OFR, representing fresh and aged peat combustion emissions, respectively. The sampling configuration is documented in Supplemental Fig. S1 with detailed sampling parameters reported by Watson et al. (2019).

2.1 $PM_{2.5}$ mass and chemical analyses

Measured chemical abundances included $PM_{2.5}$ precursor gases (i.e., nitric acid [HNO_3] and ammonia [NH_3]) as well as $PM_{2.5}$ mass and major components (e.g., elements, ions, and carbon). Water-soluble organic carbon (WSOC), carbohydrates, and organic acids that are commonly used as markers in source apportionment for biomass burning were also quantified (Chow and Watson, 2013; Watson et al., 2016).

The filter pack sampling configurations for the four upstream and two downstream channels along with filter types and analytical instrument specifications are shown in Fig. 1. Multiple sampling channels accommodate different filter substrates that allow for comprehensive chemical speciation. The additional upstream Teflon-membrane and quartz-fiber filters were taken for more specific nitrogen and organic compound analyses that are not reported here. The limited flow through the OFR precludes additional downstream sampling.

Teflon-membrane filters (i.e., channels one and five in Fig. 1) were submitted for: 1) gravimetric analysis by microbalance with ±1 μg sensitivity before and after sampling to acquire $PM_{2.5}$ mass concentrations (Watson et al., 2017); 2) filter light reflectance and transmittance by ultraviolet/visible (UV/Vis) spectrometer (200–900 nm) equipped with an integrating sphere that measures transmitted/reflected light at 1 nm interval (Johnson, 2015); 3) 51 elements (i.e., Sodium

https://doi.org/10.5194/amt-2019-198
Preprint. Discussion started: 29 May 2019

[Na] to uranium [U]) by energy-dispersive x-ray fluorescence (XRF) analysis (Watson et al., 1999); and 4) organic functional groups by Fourier Transform Infrared (FTIR) Spectrometry. Results from UV/Vis and FTIR spectrometry will be reported elsewhere.

Half of the quartz-fiber filter (i.e., channels two and six) was analyzed for: 1) four anions (i.e., chloride [CL^-], nitrite [NO_2^-], nitrate [NO_3^-], and sulfate [$SO_4^=$]), three cations (i.e., water-soluble sodium [Na^+], potassium [K^+], and ammonium [NH_4^+]), and nine organic acids (including four mono- and five di-carboxylic acids) by ion chromatography (IC) with a conductivity detector (CD) (Chow and Watson, 2017); 2) 17 carbohydrates including levoglucosan and its isomers by IC with a pulsed amperometric detector (PAD); and 3) WSOC by combustion and non-dispersive infrared (NDIR) detection. A portion (0.5 cm^2) of the other quartz-fiber filter half was analyzed for OC, EC, and brown carbon (BrC) by the IMPROVE_A multiwavelength thermal/optical reflectance/transmittance method (Chen et al., 2015; Chow et al., 2007; 2015b); the IMPROVE_A protocol (Chow et al., 2007) reports eight operationally defined thermal fractions (i.e., OC1 to OC4 evolved at 140, 280, 480, and 580 °C in helium atmosphere; EC1 to EC3 evolved at 580, 740, and 840 °C in helium/oxygen atmosphere; and pyrolyzed carbon [OP]) that further characterize carbon properties under different combustion and aging conditions. Citric acid and sodium chloride impregnated cellulose-fiber filters placed behind the Teflon-membrane and quartz-fiber filters, respectively, acquired NH_3 as NH_4^+ and HNO_3 as volatilized nitrate, respectively, with analysis by IC-CD.

Detailed chemical analyses along with quality assurance/quality control (QA/QC) measures are documented in Chow and Watson (2013). For each analysis, a minimum of 10 % of the samples were submitted for replicate analysis to estimate precisions. Precisions associated with each concentration were calculated based on error propagation (Bevington, 1969) of the analytical and sampling volume precisions (Watson et al., 2001).

2.2 $PM_{2.5}$ source profiles

Concentrations of two gases (i.e., NH_3 and HNO_3) and 125 chemical species acquired from each sample pair (fresh vs. aged) were normalized by the $PM_{2.5}$ gravimetric mass to obtain source profiles with species-specific fractional abundances. The following analyses are based on the average of 24 paired profiles (shown in Table 1), grouped by upstream (fresh) and downstream (aged) samples for 2- and 7-day aging (i.e., denoted as Fresh 2 vs. Aged 2 and Fresh 7 vs. Aged 7) for each of the six peats with 25 % fuel moisture. Composite profiles are calculated based on the

https://doi.org/10.5194/amt-2019-198
Preprint. Discussion started: 29 May 2019

average of individual abundances and the standard deviation of the average within each group (Chow et al., 2002). Although the standard deviation is termed the source profile abundance uncertainty, it is really an estimate of the profile variability for the same fuels and burning conditions, which exceeds the propagated measurement precision.

To assess changes with fuel moisture content, tests of three sets of Putnam (FL) peats at 60 % fuel moisture were conducted with resulting profiles shown in Supplemental Table S1. A few samples were voided due to filter damage or sampling abnormality, which produced five unpaired (either fresh or aged) individual profiles (Table S2). These profiles are reported as they might be useful for future source apportionment studies.

2.3 Equivalence measures

The Student *t*-test is commonly used to estimate the statistical significance of differences between chemical abundances. Two additional measures are used to determine the similarities and differences between profiles: 1) the correlation coefficient (r) between the source profile abundances (F_{ij}, the fraction of species i in peat j) divided by the source profile variabilities (σ_{ij}) that quantifies the strength of association between profiles; and 2) the distribution of weighted differences (residual [R]/uncertainty [U] = $[F_{i1} - F_{i2}]/[\sigma^2_{i1} + \sigma^2_{i2}]^{0.5}$) for $< 1\sigma$, 1σ-2σ, 2σ-3σ, and $>3\sigma$. The percent distribution of R/U ratios is used to understand how many of the chemical species differ by multiples of the uncertainty of the difference. These measures are also used in the effective variance-chemical mass balance (EV-CMB) receptor model solution that uses the variance (r^2) and the R/U ratio to quantify agreement between measured receptor concentrations and those produced by the source profiles and source contribution estimates (Watson et al., 1998).

3 Results and discussion

3.1 Similarities and differences among peat profiles

The first comparison is made between two Florida samples from locations separated by ~485 km (i.e., Putnam County Lakebed and Everglades National Park), representing different geological areas. Table S3 shows that the two profiles have high correlations (r >0.994), but are statistically different (P <0.002). Over 93 % of the chemical abundance differences fall within $\pm 3\sigma$. Statistical differences are not found when combining both fresh Florida profiles (e.g., all Fresh 2 vs. all Fresh 7), resulting in high correlations (r >0.997) with over 98 % of abundance differences within $\pm 1\sigma$ and P >0.5. However, paired comparisons of other combined profiles

https://doi.org/10.5194/amt-2019-198
Preprint. Discussion started: 29 May 2019

show statistical differences with low *P*-values (P <0.002). These two subtropical profiles should not be combined to compare with other biomes.

Similarities and differences in peat profiles by biome are summarized in Table 2. Comparisons are made for: 1) paired fresh vs. aged profiles (i.e., All Fresh vs. All Aged; Fresh 2 vs. Aged 2; Fresh 7 vs. Aged 7); 2) different experimental tests (i.e., Fresh 2 vs. Fresh 7); and 3) two aging times (i.e., Aged 2 vs. Aged 7). Equivalence measures show that most of these profiles are statistically different (P <0.05) but highly correlated (r >0.97, mostly >0.99). However, statistical differences are not found between the Fresh 2 vs. Aged 2 Malaysian profiles, which may be due to the low number of samples (n=2) in the comparison. Similar to the findings of combining both Florida profiles, fresh Alaskan and Malaysian profiles do not show statistical differences (P >0.1).

Compositing profiles by averaging each of the measured abundances may disguise some useful information. For receptor model source apportionment, region-specific profiles are most accurate for estimating source contributions.

Student *t*-tests for the gravimetric $PM_{2.5}$ mass concentrations (µg/m^3) measured upstream and downstream of the OFR (Table S4) show statistically significant differences (P <0.05) between fresh vs. aged $PM_{2.5}$ (i.e., Fresh 2 vs Aged 2 and Fresh 7 vs Aged 7). Fresh 2 and Fresh 7 $PM_{2.5}$ mass concentrations are similar, as expected from replicate tests for the same conditions. Increases in some species abundances offset decreased on other abundances, resulting in similar $PM_{2.5}$ levels for some of the fresh vs. aged comparisons.

3.2 Sum of species to $PM_{2.5}$ mass ratios

The sum of the major PM chemical abundances should be less than unity since oxygen, hydrogen, and liquid water content are not measured (Chow et al., 1994; 1996). As shown in Table S5, the sums of elements, ions, and carbon explain averages of ~70–90 % of $PM_{2.5}$ mass for fresh profiles except for Russian peat (62–64 %). The sum of species decreased by an average of 6 % and 11 % after 2- and 7-days, respectively. These differences can be attributed to loss of semi-volatile organic compounds (SVOCs), although they are offset by formation of oxygenated compounds during aging. This is true for all but Putnam (FL) peat, for which the sum of species explains nearly the same fraction of $PM_{2.5}$ for the fresh and aged profiles.

3.3 Comparison between fresh and aged profiles

Fresh and aged chemical abundances are compared in Fig. 2. Species abundances vary by over 5 orders of magnitude but exhibit two distinguishable clusters: around 0.1 % for reactive and secondary ionic species (e.g., NH_4^+, NO_3^-, and $SO_4^=$) and >1 % (mostly >10 %) for carbon compounds (e.g., OC fractions and WSOC). While most gaseous $NH_3/PM_{2.5}$ ratios exceed 10 %, $HNO_3/PM_{2.5}$ ratios are well below 1 %. Reactive/ionic species and carbon components are mostly above and below the 1:1 line, respectively, implying particle formation and evaporation after atmospheric aging. Large variabilities are found for individual species as noted by the standard deviations associated with each average.

Figure 3 shows the ratio of averages between aged and fresh profiles with increasing ratios from 2- to 7-day aging. Atmospheric aging increased oxalate, NO_3^-, NH_4^+, and $SO_4^=$ abundances (likely due to conversion of nitrogen and sulfur gases [e.g., NO, NO_2, and SO_2] to particles), but decreased NH_3, levoglucosan, and low temperature OC1 and OC2 in most cases. Large variations are found among measured species as ratios (left panels in Fig. 3) range over 7 orders of magnitude for mineral and ionic species. Consistent with Fig. 2 where most carbon compounds are close to but below the 1:1 line, the right panels in Fig. 3 show the reduction of carbonaceous abundances with ratios between 0.1 and 1 with lower ratios after 7-day aging.

Atmospheric aging should not change the abundances of mineral species (e.g., Al, Si, Ca, Ti, and Fe), except to the extent that the $PM_{2.5}$ mass (to which all species are normalized) increases or decreases with aging. Large standard deviations associated with the ratio of averages for mineral species in the left panels of Fig. 3 illustrate variabilities among different combustion tests for the less abundant species.

3.4 Carbon abundances

3.4.1 Organic carbon and thermally-evolved carbon fractions

Total carbon (TC, sum of OC and EC) constitutes the largest fraction of $PM_{2.5}$ (Table 1), accounting for 59–87 % and 43–77 % of the $PM_{2.5}$ mass for the fresh and aged profiles, respectively. Organic carbon dominates TC with low EC abundance (0.67–4.4 %), as commonly found in smoldering-dominated biomass combustion (Chakrabarty et al., 2006; Chen et al., 2007). The largest OC fractions are high temperature OC3 (15–30 % of $PM_{2.5}$), consistent with past studies for biomass burning emissions (Chen et al., 2007; Chow et al., 2004).

https://doi.org/10.5194/amt-2019-198
Preprint. Discussion started: 29 May 2019

Abundances of OC decrease with aging time. Upstream (Fresh 2 and Fresh 7) OC abundances ranged from 58–85 % and decreased by 4–12 % and 20–33 % after 2- and 7-day aging, respectively. Part, but not all of this is due to increasing abundances of non-carbon components, particularly nitrogen-containing species. The exception is for Putnam (FL) peat, where the OC abundances (67–72 %) were similar for fresh and aged profiles. OC abundance decreases after aging may have contributed to the statistical differences found between fresh and aged $PM_{2.5}$ mass (Table S4). With the exception of Putnam (FL) peat, the additional 7–22% OC degradation from 2- to 7-days implies that much of the OC changes require about a week of aging time.

The Student *t*-test for fresh and aged profiles shows statistical differences (P <0.05) for TC, OC, and low temperature OC1 and OC2, but similarities for OC3 and OC4. While the OC1 abundance is 9–18 % for fresh profiles, it decreases to 4–10 % after aging. A similar pattern is found for OC2, with 12–25 % and 9–19 % abundances for the fresh and aged profiles. The exception is Putnam (FL) peats that retained a ~20 % OC2 abundance after aging. High temperature OC3 and OC4 contain more polar and/or high molecular-weight organic components (Chen et al., 2007) that are less likely to photochemically degrade. Further reduction in OC abundances (20–33 %) after 7-days is attributed to decreases of the OC1 and OC2 in the OFR as shown in the fresh vs. aged ratios of average abundances (Fig. 3). Large fractions of pyrolized carbon (OP of 7–13 %) are also found --indicative of higher molecular-weight compounds that are likely to char (Chow et al., 2001; Chow et al., 2004; Chow et al., 2018).

3.4.2 Organic mass (OM) and OM/OC ratios

Reduction of the "sum of species" and OC abundances from fresh to aged profiles can be offset by the formation of oxygenated organic compounds as the profiles age. Different assumptions have been used to transform OC to organic mass (OM) to account for unmeasured H, O, N, and S in organic compounds (Cao, 2018; Chow et al., 2015a; Riggio et al., 2018). As single multipliers for OC cannot capture changes by oxidation in the OFR, OM is calculated by subtracting mineral components (using the IMPROVE soil formula by Malm et al. (1994)), major ions (i.e., NH_4^+, NO_3^-, and $SO_4^=$), and EC from $PM_{2.5}$ mass to account for unmeasured mass in organic compounds (Chow et al., 2015a; Frank, 2006). This approach assumes that no major chemical species are unmeasured and that the remaining mass consists of H, O, N, and S associated with OC in forming OM.

Table 3 shows that averaged OM/OC ratios are ~1.3 for fresh profiles and increases by 12–19 % from 2- to 7-days aging. These fresh OM/OC ratios are consistent with those reported for other types of biomass burning (Chen et al., 2007; Reid et al., 2005). The increased OM/OC ratios with aging are likely due to an increase in oxygenated organics. The OM/OC ratio of 1.20 ± 0.05 for fresh Borneo, Malaysian peat is consistent with the 1.26 ± 0.04 ratio for fresh peat burning aerosol in Central Kalimantan, Indonesia (Jayarathne et al., 2018), both located on the Island of Borneo.

The highest OM/OC ratios are found for Russian peat, ranging 1.6–1.7 for fresh profiles and increasing to 2.1–2.2 for aged profiles, consistent with formation of low vapor pressure oxygenated compounds in the OFR. Watson et al. (2019) report that the Russian peat fuel contains the lowest carbon (44.20 ± 1.01 %) and highest oxygen (38.64 ± 0.78 %) contents among the six peats. The low carbon contents are consistent with the lowest "sum of species" found in Russian peat, with 62–64 % and 50–52 % of $PM_{2.5}$ mass for the fresh and aged profiles, respectively. After 7-day aging for Siberian peat, the increasing OM/OC ratios from 1.2 ± 0.14 to 1.5 ± 0.18 are similar to the increase from 1.22 to 1.42 reported by Bhattarai et al. (2018).

3.4.3 Water-soluble organic carbon (WSOC)

WSOC abundances in $PM_{2.5}$ was >2-fold higher in fresh Russian (37.0 ± 2.7 %) than Malaysian (14.6 ± 0.9 %) peat. The 15–17 % WSOC in $PM_{2.5}$ for fresh Borneo, Malaysian peat (Table 1) is consistent with the 16 ± 11 % from Central Kalimantan, Indonesia peat (Jayarathne et al., 2018).

The WSOC/OC ratios also vary (Table 3), ranging from 0.18–0.64 and 0.31–0.71 for fresh and aged profiles, respectively. Russian peat OC emissions are largely water-soluble, whereas Malaysian peat emissions are mostly water-insoluble, with WSOC/OC ratios of 0.59–0.71 and 0.18–0.40, respectively. Longer aging time results in higher WSOC/OC ratios with 2–13 % and 5–19 % increases for 2- and 7-day aging.

3.4.4 Carbohydrates

Bates et al. (1991) found that peat from Sumatra, Indonesia consists of 18–46 % carbohydrate (mainly levoglucosan) relative to total carbon based on nuclear magnetic resonance spectroscopy. Levoglucosan and its isomers (mannosan and galactosan) are saccharide derivatives formed from incomplete combustion of cellulose and hemi-cellulose (Kuo et al., 2008; Louchouarn et al., 2009) and have been used as markers for biomass burning in receptor model

https://doi.org/10.5194/amt-2019-198
Preprint. Discussion started: 29 May 2019

source apportionment (Bates et al., 1991; Watson et al., 2016). These carbohydrate-derived pyrolysis products undergo heterogeneous oxidation when exposed to OH radicals in the OFR (Hennigan et al., 2010; Kessler et al., 2010).

Only five of the 17 carbohydrates (Table 1) were detected with noticeable variations (e.g., >2 orders of magnitude) in levoglucosan for boreal and temperate peats. Levoglucosan abundances account for 35–39 % and 20–25 % of $PM_{2.5}$ mass for fresh and aged Russian profiles, respectively. On a carbon basis, Table 3 shows that levoglucosan-carbon (with an OM/OC ratio of 2.25) accounts for 43–48 % and 30–35 % of WSOC and 27–28 % and 21–24 % of OC for fresh and aged Russian profiles, respectively. These levels are less than the 96 ± 3.8 % levoglucosan or ~42.7 % of levoglucosan-carbon in OC reported for German and Indonesian peats (Iinuma et al., 2007). Elevated levoglucosan is also found for Siberian and Alaskan peats, ranging from 4–18 % in $PM_{2.5}$. However, the levoglucosan abundances are reduced to 1–4 % for the subtropical and tropical peats. The 7-day aging time resulted in an additional 1–4 % levoglucosan degradation relative to 2 days with the exception of a 9 % reduction for Russian peat.

The extent of levoglucosan degradation depends on organic aerosol composition, OH exposure in the OFR, and vapor-wall losses (Bertrand et al., 2018a; 2018b; Pratap et al., 2019). Figure 4 shows the presence of 11 % and 7.6 % levoglucosan-carbon for the Russian and Alaskan peats after 2-day aging, in line with a chemical lifetime longer than 2 days. This is consistent with the estimated 1.2–3.9 days of levoglucosan lifetimes under different environments reported by Lai et al. (2014). However, other studies (Hennigan et al., 2010; May et al., 2012; Pratap et al., 2019) found that levoglucosan experiences rapid gas-phase oxidation, resulting in ~1–2 day lifetimes at ambient temperatures.

Among the carbohydrates, Jayarathne et al. (2018) reported 4.6 ± 4.0 % of levoglucosan in OC for fresh Indonesia peat. Converting to levoglucosan-carbon in Jayarathne et al. (2018) yields a fraction of 2 %, consistent with findings for Malaysian peat (1.4–2.4 %) in this study.

While the presence of levoglucosan in peat smoke is apparent, its isomer, galactosan was not detectable. Mannosan is detectable in cold climate peats with 1–5 % in $PM_{2.5}$ for the Russian and Alaskan peats and up to 1.3 % for Siberian peat. Apparent degradations from 3.9 to 2.5 % and from 5.0 to 2.1 % in mannosan abundances are found for Russian peat (Table 1) after 2- and 7-days, respectively. A 2- to 3-fold reduction in mannosan is also shown after 7 days for the Siberian and Alaskan peats. Similar observations apply to glycerol in Russian peat, ranging 1.9–3.5 % and

https://doi.org/10.5194/amt-2019-198
Preprint. Discussion started: 29 May 2019

1.3–1.7 % in $PM_{2.5}$ for fresh and aged profiles, respectively. Other detectable carbohydrates are galactose and mannitol, typically present at one hundredth of one percent of the levoglucosan abundance.

3.4.5 Organic acids

Organic acids have been associated with a mixture of anthropogenic sources, including engine exhaust, biomass burning, meat cooking, bioaerosol, and biogenic emissions. Past studies show the presence of low molecular-weight dicarboxylic acids in biomass burning emissions (e.g., Cao et al., 2016; Falkovich et al., 2005; Veres et al., 2010).

Only four of the ten measured organic acids (Table 1) in their anion forms (i.e., proprionate, oxalate, acetate, and formate) are detectable with variable abundances (<0.02–3.9 %). The largest changes between fresh and aged profiles are found for oxalate, ranging from <0.02–0.43 % of $PM_{2.5}$ for fresh profiles, with ~10- to 20-fold increase after 2 days (0.6–1.3 %), and with 1 to 2 orders of magnitude increases after 7 days (1.1–3.9 %). With the exception of Putnam, FL peat (1.1 ± 0.19 %), oxalate accounts for >2.9 % of $PM_{2.5}$ mass after 7 days.

Acetate abundances are stable between fresh and aged profiles, mostly in the range of 0.2–0.5 % except for a 6-fold increase from 0.23 ± 0.15 % (Fresh 7) to 1.5 ± 2.0 % (Aged 7) for Siberian peat with large variability among the tests. Propionate and formate abundances are low (<0.02 and <0.5 %, respectively), but increase with aging. Extending the aging time from 2- to 7-days resulted in a notable increase in organic acid abundances, consistent with the increases in WSOC/OC ratios (Table 3). By biome, the highest abundances for organic acids in $PM_{2.5}$ are found for aged (Aged 7) Siberian peat, with 3.9 ± 1.4 % oxalate, 1.5 ± 2.0 % acetate, and 0.44 ± 0.28 % formate (Table 1).

3.5 Nitrogen species, sulfate, and chloride abundances

Ammonia normalized to $PM_{2.5}$ mass is high for fresh profiles, ranging 17–64 %, except for the low NH_3 content in Russian peat (6–8 %). These abundances are reduced to 3–14 % and 1–7 % after 2- and 7-day aging, respectively. As shown in Fig. 5, most of the NH_3 rapidly diminished after 2 days, with increasing particle-phase NH_4^+ and NO_3^- after 7 days. The highest NH_3 to $PM_{2.5}$ ratios are found for fresh Everglades (FL) peat profiles (51–64 %), ~2–8 fold higher than other peats. These high and low $NH_3/PM_{2.5}$ ratios are consistent with the nitrogen contents in peat fuel: 3.93 ± 0.08 % for Everglades and 1.50 ± 0.52 % for Russian peats (Watson et al., 2019).

https://doi.org/10.5194/amt-2019-198
Preprint. Discussion started: 29 May 2019

Ionic abundances are typically <0.5 %, especially in fresh profiles. Abundances of NH_4^+ in $PM_{2.5}$ are low (0.0005–0.13 %) for fresh emissions, but increase to 0.05–1.0 % after 2 days and 3.4–6.7 % after 7 days, with the exception of Putnam (FL) peat (1.01 ± 0.05 % NH_4^+). Extending the aging time from 2- to 7-days results in an increase to ~1–7 % in NH_4^+ abundances, in contrast to NH_3 that is largely depleted after 2 days.

Figure 5b shows increasing in NO_3^- abundances with aging, 0.04–0.23 % for fresh profiles, increasing to 0.74–2.64 % after 2 days, and to 2.0–8.2 % after 7 days with the exception of Putnam (FL) peat (1.10 ± 0.18 % NO_3^-). After 7 days, NH_4^+ and NO_3^- account for ~4–7 % and ~8 % of $PM_{2.5}$ mass, respectively, for Siberian, Alaskan, and Everglades (FL) peats. No specific trend is evident for NO_2^-, mostly <0.002 % with ~0.2 % for some fresh Siberian and Alaskan peats. The ratio of gaseous HNO_3 to $PM_{2.5}$ is low, in the range of 0.2–0.5 % without much changes between fresh and aged profiles. HNO_3 created through photochemistry is largely neutralized by the abundant NH_3 in the emissions, resulting in the increasing NH_4^+ and NO_3^- to $PM_{2.5}$ in aged profiles.

The reaction of NH_3 with HNO_3 to form ammonium nitrate (NH_4NO_3) is the main pathway for inorganic aerosol formation, owing to low sulfur content in the peat fuels (Watson et al., 2019). $SO_4^=$ abundance is low in fresh profiles (0.13–1.4 %), but it increases by 2–3 fold after 2 days except for the Alaskan (0.35–0.46 %) and Everglades (FL) (1.3–1.4 %) profiles. More apparent changes are found for 7 days with the largest increase in $SO_4^=$ from 0.13 to 1.96 % for the Malaysian peats –indicating formation of ammonium sulfate ($[NH_4]_2SO_4$). The ion balance shows more NH_4^+ than needed to completely neutralize NO_3^- and $SO_4^=$ (Chow et al., 1994). Some NH_4^+ may be present as ammonium chloride (NH_4Cl), however, the abundance of chloride (Cl^-) is low (<0.3 %). The large increase in NO_3^- and $SO_4^=$ after 7 days implies that a 2-day aging time is not sufficient to allow the full formation of secondary NH_4NO_3 and $(NH_4)_2SO_4$.

3.6 Mass reconstruction

Mass reconstruction is applied to understand the changes in major chemical composition between the fresh and aged profiles. As shown in Fig. 6, the largest component in $PM_{2.5}$ is OM, accounting for 94–99 % and 80–95 % of $PM_{2.5}$ mass for fresh and aged profiles, respectively. Although the 7-day aging time increased the OM to OC ratios (by 12–19 %), the abundances of OM in $PM_{2.5}$ are reduced (3–18 %). This indicates that volatilization becomes a significant loss mechanism for SVOCs (Smith et al., 2009). The reduction of OM abundance is also partially due to increased ionic species (i.e., sum of NH_4^+, NO_3^-, and $SO_4^=$), with low abundances (0.3–1.7 %)

in fresh profiles, increasing to 3–16 % after aging. The sum of ionic species accounts for 11–16 % of $PM_{2.5}$ mass for the Siberian, Alaskan, Everglades (FL), and Malaysian peats after 7 days, mainly due to the increase in NH_4^+ and NO_3^- as shown in Fig. 5.

Elemental abundances are low (<0.0001 %), mostly below the lower quantifiable limits. Table 1 only lists 34 of the 51 elements (Na to U) detected by XRF. Using the IMPROVE soil formula (assuming metal oxides of major mineral species) yielded 0.07–2.9 % of mineral components.

This study indicates that an aging time of ~2 days represents the intermediate profile, whereas 7 days represents the profile with adequate residence time to complete the atmospheric process.

3.7 Changes in source profiles by fuel moisture content

The effect of fuel moisture content on source profiles is mostly unknown. The 25 % fuel moisture content selected for this study intends to better simulate the conditions of moderate to severe droughts where most peat fires occur. Increasing fuel moisture content from ~25 to 60 % for the three Putnam (FL) peat fuels yielded 12 % higher EFs for CO_2 (EF_{CO_2}), but 12–20 % lower EFs for CO, NO, NO_2, and $PM_{2.5}$ mass (Watson et al., 2019). Tests of fuel-moisture content on profile changes are available for only 2-day aging. Equivalence measures (Table S6) show statistical differences (P <0.001) between 25 % and 60 % moisture profiles on either fresh or aged profiles with over 93 % of species abundance fall within $\pm 3\sigma$ and high correlations (r >0.997). While OC abundances in $PM_{2.5}$ are comparable for the fresh and aged profiles (70–72 %) for 25 % fuel moisture, a reduction of 18 % OC in $PM_{2.5}$ is found for 60 % fuel moisture (from 82 to 64 %) after aging (Table S1). The higher fuel moisture content also reduced WSOC by 6 % and levoglucosan by 1.3 % with <1 % increases for NH_4^+ and organic acids. After aging, the NH_3 to $PM_{2.5}$ ratios reduced from 28 to 5 % and from 20 to 8 % for the 25 % and 60 % fuel moisture, respectively. These results are not conclusive as most measurements are associated with high variabilities.

4 Summary and conclusion

Fresh and aged peat fire emission profiles from laboratory combustion chamber and potential aerosol mass-oxidation flow reactor (PAM-OFR) for six types of peats representing boreal (Odintsovo, Russia and Pskov, Siberia), temperate (Northern Alaska, USA), subtropical (Putnam County Lakebed and Everglades National Park, Florida, USA), and tropical (Borneo,

https://doi.org/10.5194/amt-2019-198
Preprint. Discussion started: 29 May 2019

Atmospheric Measurement Techniques Discussions

Malaysia) biomes are compared. Analyses are focused on the average of 24 paired profiles grouped by six peats and by fresh vs. aged profiles for 2- and 7-days of simulated atmospheric aging.

Equivalence measures show that these profiles are highly correlated (r >0.97, mostly >0.99) but statistically different (P <0.05) between different biomes, suggesting that these profiles should be used independently for receptor model source apportionment studies in different climate regions.

The sum of chemical species (i.e., elements, ions, and carbon) explains an average of ~70–90 % of $PM_{2.5}$ mass for fresh profiles except for Russian peat (62–64 %), confirming that major $PM_{2.5}$ chemical species are measured. Aging times of 2- and 7-days resulted in an average mass depletion of 6 % and 11 %, respectively. These differences are caused by: 1) loss of SVOCs with aging, as indicated by lower abundances of OC1 and OC2 (evolved at 140 and 280 °C) in the aged profiles; and 2) replacement of the lost OC mass with unmeasured oxygen associated within secondary organic aerosol formation in the OFR.

Species abundances in $PM_{2.5}$ between aged and fresh profiles varied by >5 orders of magnitude but exhibited two distinguishable clusters, with reactive/ionic species (e.g., NH_4^+, $SO_4^=$, oxalate, and HNO_3) constituting 0.1–1 % and carbon compounds (e.g., organic carbon fractions [OC1–OC4], WSOC, and OC) constituting >1 % (mostly >10 %) of $PM_{2.5}$ mass. Most $NH_3/PM_{2.5}$ ratios are >10 % whereas $HNO_3/PM_{2.5}$ ratios are <1 %.

Total carbon (TC, sum of OC and EC) is the largest component, accounting for 59–87 % and 43–77 % of the $PM_{2.5}$ mass for the fresh and aged profiles, respectively. With predominant smoldering combustion, the majority of the TC is in OC, with low EC abundances (0.67–4.4 %). Further degradation in OC abundances (7–22 %) from 2- to 7-days implies the incomplete volatilization with short aging time. Different thermal carbon fractions are used to characterize combustion and aging conditions. While most of OC evolved at high temperatures (OC3 at 480 °C), losses of low temperature OC1 and OC2 are found, suggesting a shift of gas-particle partitioning of SVOC to gas-phase, where particle volatilization, the loss mechanism, outweighed gas-to-particle conversion.

Formation of oxygenated compounds is pronounced after aging, with organic mass (OM) to OC ratios increasing by 12–19 % from 2- to 7-days aging. The WSOC abundance in $PM_{2.5}$

varies from 14.6 ± 0.9 % to 51 ± 32 % for fresh Malaysian and Siberian peats, respectively. While levoglucosan accounts for ~1–4 % of $PM_{2.5}$ mass for fresh subtropical and tropical peats, elevated levels (~10 %) are found for boreal and temperate peats. Increasing the atmospheric aging time from 2- to 7-days results in additional formation of ionic species (e.g., oxalate, NO_3^-, NH_4^+, and $SO_4^=$), but enhanced losses of NH_3, levoglucosan, and low temperature OC1 and OC2.

Among the four climate regions, Russian peat with the lowest carbon (44 %) and highest oxygen (39 %) content, resulted in ~59–71 % of WSOC in OC along with the highest levoglucosan (20–39 % of $PM_{2.5}$) and lowest $NH_3/PM_{2.5}$ ratios (3–8 %). It also yielded the highest oxygenated compounds after aging with OM/OC ratios of 2.1–2.2. This contrasts with Malaysian peats that are mostly water-insoluble (WSOC/OC of 0.18–0.4) with low oxygenated compounds after aging (OM/OC ratios of 1.3–1.5). Large increases are found for oxalate abundances from fresh (<0.02–0.43 %) to 7-day aging (1–4%).

With the exception of Russian peats, fresh profiles contain high $NH_3/PM_{2.5}$ ratios (17–64 %) with low abundances after aging (3–14 % for Aged 2 and 1–7 % for Aged 7). Extending the aging time from 2- to 7-days results in an increase to ~7–8 % NH_4^+ and NO_3^- abundances. Although the week-long aging time increased the OM/OC ratios, abundances of OM in $PM_{2.5}$ were reduced by 3–18 % with more degradation after 7 days.

Source profiles can change with aging during transport from source to receptor. This study shows significant differences between fresh and aged peat combustion profiles between the four biomes that can be used to establish speciated emission inventories for air quality modeling. A sufficient aging time (~one week) is needed to allow gas-to-particle partitioning of semi-volatilized species, gas-phase oxidation, and volatilization to achieve representative source profiles for receptor-oriented source apportionment.

5 Author contribution

JCC, JGW, JC, L-WAC, and XW jointly designed the study, performed the data analyses, and prepared the manuscript. QW, JT, and SSHH carried out the peat combustion experiments. TBC and SDK assembled the database and performed the similarity and difference tests between the fresh and aged profiles.

6 Competing interests

The authors declare that there are no conflicts of interest.

7 Acknowledgements

This research was primarily supported by the National Science Foundation (NSF, AGS1464501) as well as internal funding from both the Desert Research Institute, Reno, NV, USA, and Institute of Earth Environment, Chinese Academy of Sciences, Xian, China. The authors thank Dr. Adam Watts of the Desert Research Institute in collecting the peat fuels.

8 References

Aerodyne: PAM users manual, Aerodyne Research Inc., Billerica, MA, 2019a. https://pamusersmanual.jimdo.com/

Aerodyne: Potential Aerosol Mass (PAM) oxidation flow reactor, Aerodyne Research Inc., Billerica, MA, 2019b. http://www.aerodyne.com/sites/default/files/u17/PAM%20Potential%20Aerosol%20Mass%20Reactor.pdf

Akagi, S. K., Yokelson, R. J., Wiedinmyer, C., Alvarado, M. J., Reid, J. S., Karl, T., Crounse, J. D., and Wennberg, P. O.: Emission factors for open and domestic biomass burning for use in atmospheric models, Atmos. Chem. Phys, 11, 4039-4072, 2011.

Bates, A. L., Hatcher, P. G., Lerch, H. E., Cecil, C. B., Neuzil, S. G., and Supardi: Studies of a petified angiosperm log cross-section from Indonesia by nuclear-magnetic resonance spectroscopy and analytical pyrolysis, Organic Geochemistry, 17, 37-45, 1991.

Bertrand, A., Stefenelli, G., Jen, C. N., Pieber, S. M., Bruns, E. A., Ni, H. Y., Temime-Roussel, B., Slowik, J. G., Goldstein, A. H., El Haddad, I., Baltensperger, U., Prevot, A. S. H., Wortham, H., and Marchand, N.: Evolution of the chemical fingerprint of biomass burning organic aerosol during aging, Atmos. Chem. Phys, 18, 7607-7624, 2018a.

Bertrand, A., Stefenelli, G., Pieber, S. M., Bruns, E. A., Temime-Roussel, B., Slowik, J. G., Wortham, H., Prevot, A. S. H., El Haddad, I., and Marchand, N.: Influence of the vapor wall loss on the degradation rate constants in chamber experiments of levoglucosan and other biomass burning markers, Atmos. Chem. Phys, 18, 10915-10930, 2018b.

Bevington, P. R.: Data Reduction and Error Analysis for the Physical Sciences, McGraw Hill, New York, NY, 1969.

Bhattarai, C., Samburova, V., Sengupta, D., Iaukea-Lum, M., Watts, A. C., Moosmuller, H., and Khlystov, A. Y.: Physical and chemical characterization of aerosol in fresh and aged emissions from open combustion of biomass fuels, Aerosol Sci. Technol., 52, 1266-1282, 2018.

Cao, F., Zhang, S. C., Kawamura, K., and Zhang, Y. L.: Inorganic markers, carbonaceous components and stable carbon isotope from biomass burning aerosols in Northeast China, Sci. Total Environ, 572, 1244-1251, 2016.

Cao, J.: A brief introduction and progress summary of the PM2.5 source profile compilation project in China, Aerosol Science and Engineering, 2, 43-50, 2018.

Cao, J. J., Wang, Q. Y., Tan, J., Zhang, Y. G., Wang, W. J., Zhong, B. L., Ho, S. S. H., Chen, L.-W. A., Wang, X. L., Watson, J. G., and Chow, J. C.: Evaluation of the oxidation flow reactor for particulate matter emission limit certification, Atmos. Environ., 2019. submitted, 2019.

CARB: Speciation profiles used in ARB modeling, California Air Resources Board, Sacramento, CA, 2018. http://arb.ca.gov/ei/speciate/speciate.htm

Chakrabarty, R. K., Moosmüller, H., Garro, M. A., Arnott, W. P., Walker, J., Susott, R. A., Babbitt, R. E., Wold, C. E., Lincoln, E. N., and Hao, W. M.: Emissions from the laboratory combustion of wildland fuels: Particle morphology and size, J. Geophys. Res. Atmos., 111, D07204, 2006.

Chen, L.-W. A., Chow, J. C., Wang, X. L., Robles, J. A., Sumlin, B. J., Lowenthal, D. H., Zimmermann, R., and Watson, J. G.: Multi-wavelength optical measurement to enhance thermal/optical analysis for carbonaceous aerosol, Atmos. Meas. Tech., 8, 451-461, 2015.

Chen, L.-W. A., Moosmüller, H., Arnott, W. P., Chow, J. C., Watson, J. G., Susott, R. A., Babbitt, R. E., Wold, C. E., Lincoln, E. N., and Hao, W. M.: Emissions from laboratory combustion of wildland fuels: Emission factors and source profiles, Environ. Sci. Technol., 41, 4317-4325, 2007.

https://doi.org/10.5194/amt-2019-198
Preprint. Discussion started: 29 May 2019

Atmospheric Measurement Techniques Discussions

Chow, J. C., Engelbrecht, J. P., Watson, J. G., Wilson, W. E., Frank, N. H., and Zhu, T.: Designing monitoring networks to represent outdoor human exposure, Chemosphere, 49, 961-978, 2002.

Chow, J. C., Fujita, E. M., Watson, J. G., Lu, Z., Lawson, D. R., and Ashbaugh, L. L.: Evaluation of filter-based aerosol measurements during the 1987 Southern California Air Quality Study, Environ. Mon. Assess, 30, 49-80, 1994.

Chow, J. C., Lowenthal, D. H., Chen, L.-W. A., Wang, X. L., and Watson, J. G.: Mass reconstruction methods for $PM_{2.5}$: A review, Air Qual. Atmos. Health, 8, 243-263, 2015a.

Chow, J. C., Riggio, G. M., Wang, X. L., Chen, L.-W. A., and Watson, J. G.: Measuring the organic carbon to organic matter multiplier with thermal/optical carbon mass spectrometer analyses, Aerosol Science and Engineering, 2, 165-172, 2018.

Chow, J. C., Wang, X. L., Sumlin, B. J., Gronstal, S. B., Chen, L.-W. A., Trimble, D. L., Kohl, S. D., Mayorga, S. R., Riggio, G. M., Hurbain, P. R., Johnson, M., Zimmermann, R., and Watson, J. G.: Optical calibration and equivalence of a multiwavelength thermal/optical carbon analyzer, Aerosol Air Qual. Res., 15, 1145-1159, 2015b.

Chow, J. C. and Watson, J. G.: Chemical analyses of particle filter deposits. In: Aerosols Handbook : Measurement, Dosimetry, and Health Effects, Ruzer, L. and Harley, N. H. (Eds.), CRC Press/Taylor & Francis, New York, NY, 2013.

Chow, J. C. and Watson, J. G.: Enhanced ion chromatographic speciation of water-soluble $PM_{2.5}$ to improve aerosol source apportionment, Aerosol Science and Engineering, 1, 7-24, 2017.

Chow, J. C., Watson, J. G., Chen, L.-W. A., Arnott, W. P., Moosmüller, H., and Fung, K. K.: Equivalence of elemental carbon by Thermal/Optical Reflectance and Transmittance with different temperature protocols, Environ. Sci. Technol., 38, 4414-4422, 2004.

Chow, J. C., Watson, J. G., Chen, L.-W. A., Chang, M.-C. O., Robinson, N. F., Trimble, D. L., and Kohl, S. D.: The IMPROVE_A temperature protocol for thermal/optical carbon analysis: Maintaining consistency with a long-term database, J. Air Waste Manage. Assoc., 57, 1014-1023, 2007.

Chow, J. C., Watson, J. G., Crow, D., Lowenthal, D. H., and Merrifield, T. M.: Comparison of IMPROVE and NIOSH carbon measurements, Aerosol Sci. Technol., 34, 23-34, 2001.

Chow, J. C., Watson, J. G., Lu, Z., Lowenthal, D. H., Frazier, C. A., Solomon, P. A., Thuillier, R. H., and Magliano, K. L.: Descriptive analysis of $PM_{2.5}$ and PM_{10} at regionally representative locations during SJVAQS/AUSPEX, Atmos. Environ., 30, 2079-2112, 1996.

Falkovich, A. H., Graber, E. R., Schkolnik, G., Rudich, Y., Maenhaut, W., and Artaxo, P.: Low molecular weight organic acids in aerosol particles from Rondonia, Brazil, during the biomass-burning, transition and wet periods, Atmos. Chem. Phys, 5, 781-797, 2005.

Frank, N. H.: Retained nitrate, hydrated sulfates, and carbonaceous mass in Federal Reference Method fine particulate matter for six eastern cities, J. Air Waste Manage. Assoc., 56, 500-511, 2006.

Hennigan, C. J., Sullivan, A. P., Collett Jr., J. L., and Ronbinson, A. L.: Levoglucosan stability in biomass burning particles exposed to hydroxyl radicals, Geophysical Research Letters, 37, 1-4, 2010.

Hidy, G. M. and Friedlander, S. K.: The nature of the Los Angeles aerosol. In: Proceedings, Second International Clean Air Congress, Englund, H. M. and Beery, W. T. (Eds.), Academic Press, New York, 1971.

Hu, Y. Q., Fernandez-Anez, N., Smith, T. E. L., and Rein, G.: Review of emissions from smouldering peat fires and their contribution to regional haze episodes, International Journal of Wildland Fire, 27, 293-312, 2018.

Iinuma, Y., Bruggemann, E., Gnauk, T., Muller, K., Andreae, M. O., Helas, G., Parmar, R., and Herrmann, H.: Source characterization of biomass burning particles: The combustion of selected European conifers, African hardwood, savanna grass, and German and Indonesian peat, J. Geophys. Res. Atmos., 112, 2007.

Jayarathne, T., Stockwell, C. E., Gilbert, A. A., Daugherty, K., Cochrane, M. A., Ryan, K. C., Putra, E. I., Saharjo, B. H., Nurhayati, A. D., Albar, I., Yokelson, R. J., and Stone, E. A.: Chemical characterization of fine particulate matter emitted by peat fires in Central Kalimantan, Indonesia, during the 2015 El Nino, Atmos. Chem. Phys, 18, 2585-2600, 2018.

Jimenez, J. L.: Oxidation flow reactors (including PAM): Principles and best practices for applications in aerosol research, 2018 International Aerosol Conference Tutorial, St. Louis, MO, 2018. https://docs.google.com/viewer?a=v&pid=sites&srcid=ZGVmYXVsdGRvbWFpbnxwYW13aWtpfGd4OjY0N2MyYTZkYThiODU0MTM

Johnson, M. M.: Evaluatoin of a multiwavelength characterization of brown and black carbon from filter samples, M.S. Thesis, University of Nevada, Reno, Reno, NV, 2015.

Kang, E., Root, M. J., Toohey, D. W., and Brune, W. H.: Introducing the concept of Potential Aerosol Mass (PAM), Atmos. Chem. Phys, 7, 5727-5744, 2007.

Kessler, S. H., Smith, J. D., Che, D. L., Worsnop, D. R., Wilson, K. R., and Kroll, J. H.: Chemical sinks of organic aerosol: Kinetics and products of the heterogeneous oxidation of erythritol and levoglucosan, Environ. Sci. Technol., 44, 7005-7010, 2010.

Kuo, L. J., Herbert, B. E., and Louchouarn, P.: Can levoglucosan be used to characterize and quantify char/charcoal black carbon in environmental media?, Organic Geochemistry, 39, 1466-1478, 2008.

Lai, C. Y., Liu, Y. C., Ma, J. Z., Ma, Q. X., and He, H.: Degradation kinetics of levoglucosan initiated by hydroxyl radical under different environmental conditions, Atmos. Environ., 91, 32-39, 2014.

Lambe, A. T., Ahern, A. T., Williams, L. R., Slowik, J. G., Wong, J. P. S., Abbatt, J. P. D., Brune, W. H., Ng, N. L., Wright, J. P., Croasdale, D. R., Worsnop, D. R., Davidovits, P., and Onasch, T. B.: Characterization of aerosol photooxidation flow reactors: heterogeneous oxidation, secondary organic aerosol formation and cloud condensation nuclei activity measurements, Atmos. Meas. Tech., 4, 445-461, 2011.

Liu, Y. Y., Zhang, W. J., Bai, Z. P., Yang, W., Zhao, X. Y., Han, B., and Wang, X. H.: China Source Profile Shared Service (CSPSS): The Chinese $PM_{2.5}$ database for source profiles, Aerosol Air Qual. Res., 17, 1501-1514, 2017.

Louchouarn, P., Kuo, L. J., Wade, T. L., and Schantz, M.: Determination of levoglucosan and its isomers in size fractions of aerosol standard reference materials, Atmos. Environ., 43, 5630-5636, 2009.

Malm, W. C., Trijonis, J. C., Sisler, J. F., Pitchford, M. L., and Dennis, R. L.: Assessing the effect of SO_2 emission changes on visibility, Atmos. Environ., 28, 1023-1034, 1994.

May, A. A., Saleh, R., Hennigan, C. J., Donahue, N. M., and Robinson, A. L.: Volatility of organic molecular markers used for source apportionment analysis: Measurements and implications for atmospheric lifetime, Environ. Sci. Technol., 46, 12435-12444, 2012.

Mo, Z. W., Shao, M., and Lu, S. H.: Compilation of a source profile database for hydrocarbon and OVOC emissions in China, Atmos. Environ., 143, 209-217, 2016.

Nara, H., Tanimoto, H., Tohjima, Y., Mukai, H., Nojiri, Y., and Machida, T.: Emission factors of CO2, CO and CH4 from Sumatran peatland fires in 2013 based on shipboard measurements, Tellus Series B-Chemical and Physical Meteorology, 69, 2017.

https://doi.org/10.5194/amt-2019-198
Preprint. Discussion started: 29 May 2019

Atmospheric Measurement Techniques Discussions

Pernigotti, D., Belis, C. A., and Spanò, L.: SPECIEUROPE: The European data base for PM source profiles, Atmospheric Pollution Research, 7, 307-314, 2016.

Pratap, V., Bian, Q. J., Kiran, S. A., Hopke, P. K., Pierce, J. R., and Nakao, S.: Investigation of levoglucosan decay in wood smoke smog-chamber experiments: The importance of aerosol loading, temperature, and vapor wall losses in interpreting results, Atmos. Environ., 199, 224-232, 2019.

Reid, J. S., Eck, T. F., Christopher, S. A., Koppmann, R., Dubovik, O., Eleuterio, D. P., Holben, B. N., Reid, E. A., and Zhang, J.: A review of biomass burning emissions part III: intensive optical properties of biomass burning particles, Atmos. Chem. Phys, 5, 827-849, 2005.

Riggio, G. M., Chow, J. C., Cropper, P. M., Wang, X. L., Yatavelli, R. L. N., Yang, X. F., and Watson, J. G.: Feasibility of coupling a thermal/optical carbon analyzer to a quadrupole mass spectrometer for enhanced $PM_{2.5}$ speciation, J. Air Waste Manage. Assoc., 68, 463-476, 2018.

Smith, J. D., Kroll, J. H., Cappa, C. D., Che, D. L., Liu, C. L., Ahmed, M., Leone, S. R., Worsnop, D. R., and Wilson, K. R.: The heterogeneous reaction of hydroxyl radicals with sub-micron squalane particles: a model system for understanding the oxidative aging of ambient aerosols, Atmos. Chem. Phys, 9, 3209-3222, 2009.

Stockwell, C. E., Jayarathne, T., Cochrane, M. A., Ryan, K. C., Putra, E. I., Saharjo, B. H., Nurhayati, A. D., Albar, I., Blake, D. R., Simpson, I. J., Stone, E. A., and Yokelson, R. J.: Field measurements of trace gases and aerosols emitted by peat fires in Central Kalimantan, Indonesia, during the 2015 El Nino, Atmos. Chem. Phys, 16, 11711-11732, 2016.

Stockwell, C. E., Yokelson, R. J., Kreidenweis, S. M., Robinson, A. L., Demott, P. J., Sullivan, R. C., Reardon, J., Ryan, K. C., Griffith, D. W. T., and Stevens, L.: Trace gas emissions from combustion of peat, crop residue, domestic biofuels, grasses, and other fuels: configuration and Fourier transform infrared (FTIR) component of the fourth Fire Lab at Missoula Experiment (FLAME-4), Atmos. Chem. Phys, 14, 9727-9754, 2014.

U.S.EPA: Guidance on the use of models and other analyses for demonstrating attainment of air quality goals for ozone, PM2.5, and regional haze, U.S. Environmental Protection Agency, Research Triangle Park, NC, 2007. http://www.epa.gov/ttn/scram/guidance/guide/final-03-pm-rh-guidance.pdf

U.S.EPA: SPECIATE Version 4.5, U.S. Environmental Protection Agency, Research Triangle Park, NC, 2016. https://www.epa.gov/air-emissions-modeling/speciate-version-45-through-40

Veres, P., Roberts, J. M., Burling, I. R., Warneke, C., de Gouw, J., and Yokelson, R. J.: Measurements of gas-phase inorganic and organic acids from biomass fires by negative-ion proton-transfer chemical-ionization mass spectrometry, J. Geophys. Res. Atmos., 115, 2010.

Watson, J. G., Cao, J., Wang, Q., Tan, J., Li, L., Ho, S. S. H., Chen, L.-W. A., Watts, A. C., Wang, X. L., and Chow, J. C.: Gaseous, $PM_{2.5}$ mass, ans speciiated emission factors from laboratory chamber peat combustion, Atmos. Chem. Phys, 2019. submitted, 2019.

Watson, J. G., Chow, J. C., Engling, G., Chen, L.-W. A., and Wang, X. L.: Source apportionment: Principles and methods. In: Airborne Particulate Matter: Sources, Atmospheric Processes and Health, Harrison, R. M. (Ed.), Royal Society of Chemistry, London, UK, 2016.

Watson, J. G., Chow, J. C., and Frazier, C. A.: X-ray fluorescence analysis of ambient air samples. In: Elemental Analysis of Airborne Particles, Vol. 1, Landsberger, S. and Creatchman, M. (Eds.), Advances in Environmental, Industrial and Process Control Technologies, Gordon and Breach Science, Amsterdam, The Netherlands, 1999.

Watson, J. G., Chow, J. C., Wang, X. L., Kohl, S. D., Chen, L.-W. A., and Etyemezian, V. R.: Overview of real-world emission characterization methods. In: Alberta Oil Sands: Energy, Industry, and the Environment, Percy, K. E. (Ed.), Developments in Environmental Science, Elsevier Press, Amsterdam, The Netherlands, 2012.

https://doi.org/10.5194/amt-2019-198
Preprint. Discussion started: 29 May 2019

Atmospheric Measurement Techniques Discussions

Watson, J. G., Robinson, N. F., Lewis, C. W., Coulter, C. T., Chow, J. C., Fujita, E. M., Conner, T. L., and Pace, T. G.: CMB8 applications and validation protocol for $PM_{2.5}$ and VOCs, Desert Research Institute, Reno, NV, 1998. http://www.epa.gov/scram001/models/receptor/CMB_Protocol.pdf

Watson, J. G., Tropp, R. J., Kohl, S. D., Wang, X. L., and Chow, J. C.: Filter processing and gravimetric analysis for suspended particulate matter samples, Aerosol Science and Engineering, 1, 193-205, 2017.

Watson, J. G., Turpin, B. J., and Chow, J. C.: The measurement process: Precision, accuracy, and validity. In: Air Sampling Instruments for Evaluation of Atmospheric Contaminants, Ninth Edition, Cohen, B. S. and McCammon, C. S., Jr (Eds.), American Conference of Governmental Industrial Hygienists, Cincinnati, OH, 2001.

Wiggins, E. B., Czimczik, C. I., Santos, G. M., Chen, Y., Xu, X. M., Holden, S. R., Randerson, J. T., Harvey, C. F., Kai, F. M., and Yu, L. E.: Smoke radiocarbon measurements from Indonesian fires provide evidence for burning of millennia-aged peat, Proceedings of the National Academy of Sciences of the United States of America, 115, 12419-12424, 2018.

https://doi.org/10.5194/amt-2019-198
Preprint. Discussion started: 29 May 2019

Atmospheric Measurement Techniques
Discussions

Table 1. Fresh and aged average profiles (in % of $PM_{2.5}$ mass) for six types of peats

	Average ± Standard Deviation of Percent $PM_{2.5}$ Mass[a]							
	Boreal							
	Odintsovo, Russia				Pskov, Siberia			
Aging Time	2 days		7 days		2 days		7 days	
	Fresh 2	Aged 2	Fresh 7	Aged 7	Fresh 2	Aged 2[b]	Fresh 7	Aged 7
Peat IDs in the average[c]	PEAT030, PEAT031, PEAT032		PEAT033, PEAT034, PEAT035		PEAT023, PEAT025, PEAT026		PEAT027, PEAT028, PEAT029	
Nitric Acid (HNO_3)	0.18 ± 0.080	0.32 ± 0.15	0.21 ± 0.059	0.24 ± 0.085	0.18 ± 0.052	0.27 ± 0.074	0.27 ± 0.075	0.39 ± 0.15
Ammonia (NH_3)	6.0095 ± 0.93	3.21 ± 0.78	7.84 ± 0.31	4.56 ± 1.36	18.21 ± 3.97	8.81 ± 4.047	22.81 ± 5.88	7.090 ± 5.59
Water-Soluble Sodium (Na^+)	0.018 ± 0.0015	0.024 ± 0.0013	0.022 ± 0.011	0.032 ± 0.0074	0.017 ± 0.0011	0.047 ± 0.020	0.0688 ± 0.038	0.058 ± 0.053
Water-Soluble Potassium (K^+)	0.034 ± 0.036	na[d]	0.11 ± 0.087	na[d]	0.020 ± 0.016	na[d]	0.0230 ± 0.014	na[d]
Chloride (Cl^-)	0.16 ± 0.022	0.12 ± 0.019	0.25 ± 0.053	0.092 ± 0.011	0.11 ± 0.031	0.11 ± 0.048	0.17 ± 0.014	0.086 ± 0.033
Nitrite (NO_2^-)	0.037 ± 0.063	0.00095 ± 0.0016	0.00 ± 0.00028	0.00086 ± 0.00077	0.0013 ± 0.0023	0.0023 ± 0.0036	0.20 ± 0.34	0.0056 ± 0.0033
Nitrate (NO_3^-)	0.23 ± 0.20	0.74 ± 0.080	0.13 ± 0.043	2.0029 ± 0.71	0.11 ± 0.11	1.79 ± 0.52	0.15 ± 0.076	8.23 ± 4.34
Sulfate ($SO_4^{=}$)	0.30 ± 0.33	0.67 ± 0.46	0.15 ± 0.044	0.84 ± 0.24	0.28 ± 0.15	0.68 ± 0.19	0.27 ± 0.025	1.15 ± 0.63
Ammonium (NH_4^+)	0.13 ± 0.14	1.045 ± 0.93	0.097 ± 0.057	3.38 ± 1.38	0.0014 ± 0.0012	0.21 ± 0.18	0.0463 ± 0.044	6.66 ± 3.67
OC1 (140°C)	11.82 ± 2.58	6.42 ± 3.94	15.67 ± 3.60	4.096 ± 0.72	11.81 ± 2.20	5.014 ± 0.70	11.40 ± 0.65	4.34 ± 1.69
OC2 (280°C)	13.16 ± 1.42	9.84 ± 1.094	12.029 ± 1.049	9.032 ± 1.27	20.59 ± 1.87	15.45 ± 2.65	21.21 ± 2.38	10.54 ± 0.18
OC3 (480°C)	17.69 ± 3.013	14.60 ± 1.93	17.33 ± 2.39	13.99 ± 2.46	25.93 ± 3.62	26.78 ± 8.46	29.63 ± 5.62	19.74 ± 0.79
OC4 (580°C)	6.69 ± 0.49	5.83 ± 0.51	6.090 ± 1.61	4.40 ± 0.84	5.79 ± 0.21	8.85 ± 1.27	8.72 ± 3.83	6.31 ± 2.35
Pyrolized Carbon (OP)	8.26 ± 2.086	8.61 ± 4.35	9.29 ± 1.0016	9.39 ± 1.30	9.52 ± 2.15	12.12 ± 4.27	10.34 ± 1.82	12.76 ± 1.58
Organic Carbon (OC)	57.61 ± 5.21	45.29 ± 9.90	60.42 ± 5.37	40.90 ± 4.87	73.65 ± 6.82	68.21 ± 13.33	81.30 ± 9.29	53.69 ± 5.32
EC1 (580°C)	6.47 ± 1.64	6.77 ± 2.33	6.51 ± 0.53	9.31 ± 1.50	7.84 ± 2.19	9.23 ± 0.82	5.31 ± 0.57	7.79 ± 1.28
EC2 (740°C)	3.60 ± 2.32	3.36 ± 2.52	4.61 ± 0.034	2.051 ± 0.50	4.92 ± 3.76	5.98 ± 4.73	5.87 ± 0.74	7.038 ± 2.48
EC3 (840°C)	0.00 ± 0.00020	0.00 ± 0.00022	0.00 ± 0.00020	0.00 ± 0.00021	0.00 ± 0.00021	0.00 ± 0.00028	0.00 ± 0.00029	0.00 ± 0.00032
Elemental Carbon (EC)	1.82 ± 1.26	1.52 ± 0.36	1.83 ± 0.69	1.98 ± 0.75	3.23 ± 0.80	3.090 ± 0.83	0.83 ± 1.30	2.076 ± 0.36
Total Carbon (TC)	59.43 ± 4.49	46.81 ± 10.23	62.25 ± 4.95	42.88 ± 4.76	76.88 ± 6.37	71.30 ± 13.96	82.14 ± 10.57	55.77 ± 5.58
Water-Soluble OC (WSOC)	36.97 ± 2.71	31.80 ± 3.15	35.77 ± 2.30	29.21 ± 6.31	23.84 ± 1.84	29.88 ± 7.10	32.50 ± 0.71[e]	29.88 ± 8.88
Formate ($CH_2O_2^-$)	0.17 ± 0.074	0.23 ± 0.054	0.23 ± 0.090	0.32 ± 0.18	0.045 ± 0.016	0.18 ± 0.054	0.067 ± 0.0097	0.44 ± 0.28
Acetate ($C_2H_4O_2^-$)	0.61 ± 0.38	0.63 ± 0.37	0.67 ± 0.15	0.88 ± 0.47	0.20 ± 0.16	0.34 ± 0.15	0.23 ± 0.15	1.46 ± 2.03
Oxalate ($C_2H_2O_4^{=}$)	0.10 ± 0.063	0.97 ± 0.20	0.28 ± 0.22	2.88 ± 0.77	0.062 ± 0.013	1.31 ± 0.47	0.076 ± 0.019	3.90 ± 1.43
Propionate ($C_3H_5O_2^-$)	0.036 ± 0.032	0.12 ± 0.15	0.066 ± 0.032	0.020 ± 0.031	0.00 ± 0.00015	0.026 ± 0.045	0.032 ± 0.032	0.00 ± 0.00023
Levoglucosan ($C_6H_{10}O_5$)	35.35 ± 7.90	24.95 ± 8.97	38.66 ± 2.089	19.63 ± 4.044	6.66 ± 2.58	4.21 ± 0.59	9.39 ± 2.077	3.80 ± 0.35
Mannosan ($C_6H_{10}O_5$)	3.93 ± 1.18	2.52 ± 1.068	5.039 ± 0.58	2.14 ± 0.85	0.053 ± 0.092	0.00 ± 0.00044	1.28 ± 0.54	0.46 ± 0.16
Galactose/Maltitol ($C_6H_{12}O_6$/$C_{12}H_{24}O_{11}$)	0.00 ± 0.00016	0.00 ± 0.00017	0.063 ± 0.11	0.00 ± 0.00016	0.0058 ± 0.010	0.00 ± 0.00023	0.00 ± 0.00023	0.082 ± 0.14
Glycerol ($C_3H_8O_3$)	1.90 ± 0.19	1.73 ± 0.42	3.54 ± 2.14	1.25 ± 0.17	0.00 ± 0.0000029	0.00 ± 0.0000040	0.43 ± 0.43	0.00 ± 0.0000046
Mannitol ($C_6H_{14}O_6$)	0.00 ± 0.000056	0.00 ± 0.000061	0.062 ± 0.11	0.00 ± 0.000058	0.00 ± 0.000058	0.00 ± 0.000081	0.00 ± 0.0000836	0.17 ± 0.30
Aluminum (Al)	0.073 ± 0.66	0.15 ± 0.87	0.22 ± 0.73	0.29 ± 2.74	0.086 ± 1.49	0.00 ± 0.0074	0.075 ± 0.83	0.20 ± 0.17
Silicon (Si)	0.0069 ± 0.12	0.12 ± 0.44	0.013 ± 0.12	0.68 ± 0.24	0.022 ± 0.19	0.22 ± 0.00089	0.0050 ± 0.044	0.47 ± 0.79
Phosphorous (P)	0.00 ± 0.000084	0.00018 ± 0.00025	0.00079 ± 0.0014	0.00 ± 0.000095	0.00 ± 0.000090	0.00 ± 0.00017	0.00 ± 0.00012	0.00 ± 0.000093

Table 1 (cont'd)

Sulfur (S)	0.024 ± 0.0088	0.081 ± 0.046	0.040 ± 0.056	0.26 ± 0.095	0.081 ± 0.030	0.090 ± 0.000098	0.028 ± 0.034	0.31 ± 0.0057
Chlorine (Cl)	0.12 ± 0.027	0.035 ± 0.019	0.18 ± 0.030	0.032 ± 0.0025	0.11 ± 0.015	0.057 ± 0.000068	0.081 ± 0.018	0.027 ± 0.0064
Potassium (K)	0.030 ± 0.011	0.48 ± 0.44	0.041 ± 0.018	0.13 ± 0.035	0.15 ± 0.19	0.096 ± 0.00025	0.11 ± 0.14	0.30 ± 0.017
Calcium (Ca)	0.018 ± 0.016	0.040 ± 0.056	0.031 ± 0.025	0.0034 ± 0.0048	0.00 ± 0.00	0.00 ± 0.00092	0.00 ± 0.00065	0.028 ± 0.039
Scandium (Sc)	0.064 ± 0.11	0.00 ± 0.0021	0.00 ± 0.0021	0.00 ± 0.0023	0.079 ± 0.14	0.00 ± 0.0041	0.031 ± 0.053	0.00 ± 0.0022
Titanium (Ti)	0.0046 ± 0.0056	0.00 ± 0.000076	0.0055 ± 0.0049	0.0013 ± 0.0018	0.0079 ± 0.014	0.00 ± 0.00015	0.00 ± 0.00010	0.00 ± 0.000078
Vanadium (V)	0.00 ± 0.000013	0.00 ± 0.000014	0.00 ± 0.000014	0.00 ± 0.000015	0.00070 ± 0.0012	0.00 ± 0.000027	0.00 ± 0.000019	0.00 ± 0.000015
Chromium (Cr)	0.0012 ± 0.0020	0.00039 ± 0.00056	0.00 ± 0.000046	0.00084 ± 0.0012	0.00079 ± 0.0014	0.00 ± 0.000091	0.0010 ± 0.00095	0.00 ± 0.000049
Manganese (Mn)	0.0014 ± 0.0022	0.00053 ± 0.00074	0.0037 ± 0.0033	0.00 ± 0.00018	0.0018 ± 0.0022	0.020 ± 0.00032	0.0031 ± 0.0031	0.0051 ± 0.0072
Iron (Fe)	0.038 ± 0.021	0.091 ± 0.098	0.062 ± 0.043	0.26 ± 0.32	0.039 ± 0.035	0.029 ± 0.00056	0.013 ± 0.017	0.015 ± 0.021
Cobalt (Co)	0.000032 ± 0.000056	0.00 ± 0.0000094	0.000037 ± 0.000064	0.00049 ± 0.00069	0.00018 ± 0.00031	0.00 ± 0.000018	0.00 ± 0.000013	0.00 ± 0.000018
Nickel (Ni)	0.00 ± 0.000022	0.0026 ± 0.0037	0.000029 ± 0.000050	0.00 ± 0.000025	0.00 ± 0.000024	0.00086 ± 0.000045	0.0014 ± 0.0017	0.00041 ± 0.00039
Copper (Cu)	0.0055 ± 0.0029	0.15 ± 0.11	0.0052 ± 0.0038	0.046 ± 0.054	0.0072 ± 0.0041	0.014 ± 0.00028	0.047 ± 0.052	0.11 ± 0.067
Zinc (Zn)	0.0017 ± 0.0015	0.054 ± 0.066	0.0047 ± 0.0041	0.053 ± 0.070	0.0053 ± 0.0030	0.0034 ± 0.00016	0.0058 ± 0.0056	0.0019 ± 0.00081
Arsenic (As)	0.00086 ± 0.0015	0.00 ± 0.000038	0.00 ± 0.000037	0.00 ± 0.000040	0.00076 ± 0.0013	0.0050 ± 0.000073	0.000069 ± 0.00012	0.00013 ± 0.00019
Selenium (Se)	0.00021 ± 0.00036	0.0026 ± 0.0037	0.00067 ± 0.00076	0.00029 ± 0.00041	0.0018 ± 0.0022	0.0026 ± 0.00013	0.00035 ± 0.00031	0.00029 ± 0.00041
Bromine (Br)	0.00041 ± 0.00036	0.0030 ± 0.0031	0.00096 ± 0.0014	0.0021 ± 0.0019	0.0072 ± 0.0043	0.0032 ± 0.000036	0.0092 ± 0.0066	0.0066 ± 0.0014
Rubidium (Rb)	0.00052 ± 0.00090	0.0029 ± 0.000079	0.0020 ± 0.0019	0.00049 ± 0.00069	0.00031 ± 0.00054	0.00 ± 0.000045	0.00066 ± 0.00068	0.0024 ± 0.0034
Strontium (Sr)	0.0033 ± 0.0032	0.0017 ± 0.0018	0.0032 ± 0.0027	0.0033 ± 0.0013	0.0027 ± 0.0028	0.0039 ± 0.000045	0.0072 ± 0.0042	0.0047 ± 0.0066
Yttrium (Y)	0.00079 ± 0.0013	0.000066 ± 0.000093	0.0031 ± 0.0035	0.00077 ± 0.0011	0.0014 ± 0.0012	0.0015 ± 0.000045	0.0045 ± 0.0045	0.0053 ± 0.0049
Zirconium (Zr)	0.0040 ± 0.0024	0.0034 ± 0.0014	0.0013 ± 0.0018	0.0017 ± 0.0024	0.0051 ± 0.0019	0.00 ± 0.00017	0.0060 ± 0.0088	0.0033 ± 0.0021
Niobium (Nb)	0.00072 ± 0.0012	0.0023 ± 0.0013	0.00036 ± 0.00038	0.00063 ± 0.00089	0.00040 ± 0.00069	0.00064 ± 0.000082	0.00039 ± 0.00067	0.00044 ± 0.00062
Molybdenum (Mo)	0.0020 ± 0.0035	0.00 ± 0.000090	0.0015 ± 0.0011	0.0030 ± 0.0010	0.0029 ± 0.0051	0.00 ± 0.00017	0.0013 ± 0.0022	0.0026 ± 0.0037
Silver (Ag)	0.0010 ± 0.0015	0.00 ± 0.00011	0.00 ± 0.00011	0.00 ± 0.00012	0.00 ± 0.00011	0.00 ± 0.00022	0.0083 ± 0.0074	0.00 ± 0.00012
Cadmium (Cd)	0.0034 ± 0.0059	0.0038 ± 0.0053	0.0023 ± 0.0039	0.0023 ± 0.0033	0.00 ± 0.00016	0.00 ± 0.00030	0.0024 ± 0.0029	0.00 ± 0.00016
Indium (In)	0.00 ± 0.00010	0.00 ± 0.00011	0.0059 ± 0.0011	0.0060 ± 0.0016	0.00065 ± 0.0011	0.018 ± 0.00021	0.0027 ± 0.0047	0.00 ± 0.00011
Tin (Sn)	0.0028 ± 0.0048	0.0095 ± 0.013	0.0013 ± 0.0022	0.0037 ± 0.0053	0.0098 ± 0.010	0.0075 ± 0.00038	0.0092 ± 0.014	0.0089 ± 0.013
Antimony (Sb)	0.00 ± 0.00028	0.0086 ± 0.012	0.00 ± 0.00029	0.00 ± 0.00032	0.00 ± 0.00030	0.000053 ± 0.00058	0.00 ± 0.00041	0.00 ± 0.00031
Cesium (Cs)	0.025 ± 0.040	0.0085 ± 0.012	0.023 ± 0.033	0.014 ± 0.020	0.0057 ± 0.0099	0.00 ± 0.0016	0.0046 ± 0.0079	0.00 ± 0.00086
Barium (Ba)	0.014 ± 0.024	0.00 ± 0.00071	0.011 ± 0.020	0.00 ± 0.00068	0.023 ± 0.020	0.00 ± 0.0012	0.00 ± 0.00086	0.00 ± 0.0067
Lanthanum (La)	0.048 ± 0.043	0.00 ± 0.0012	0.049 ± 0.043	0.059 ± 0.083	0.017 ± 0.030	0.00 ± 0.0024	0.094 ± 0.085	0.020 ± 0.028
Wolfram (W)	0.0023 ± 0.0014	0.0073 ± 0.010	0.0077 ± 0.013	0.011 ± 0.0016	0.00079 ± 0.0014	0.00 ± 0.00047	0.0047 ± 0.0082	0.0048 ± 0.00054
Gold (Au)	0.0029 ± 0.0027	0.00 ± 0.000071	0.00080 ± 0.0014	0.0024 ± 0.0033	0.00 ± 0.000071	0.012 ± 0.00014	0.0038 ± 0.0065	0.0018 ± 0.0025
Mercury (Hg)	0.0015 ± 0.0014	0.00 ± 0.000038	0.00081 ± 0.0014	0.00 ± 0.000040	0.0013 ± 0.0023	0.00 ± 0.000073	0.000065 ± 0.00011	0.00 ± 0.000039
Lead (Pb)	0.0026 ± 0.0024	0.0018 ± 0.0025	0.0024 ± 0.0028	0.0053 ± 0.0074	0.00 ± 0.000071	0.00 ± 0.00014	0.0050 ± 0.00088	0.0027 ± 0.0032
Uranium (U)	0.0018 ± 0.0031	0.0017 ± 0.0024	0.00096 ± 0.0017	0.0024 ± 0.0035	0.0028 ± 0.0027	0.00 ± 0.00025	0.0025 ± 0.0033	0.0046 ± 0.0066

https://doi.org/10.5194/amt-2019-198
Preprint. Discussion started: 29 May 2019

Table 1 (cont'd)

	Average ± Standard Deviation of Percent $PM_{2.5}$ Mass							
	Temperate				Subtropical			
	Northern Alaska, USA				Putnam County Lakebed, Florida			
Aging Time	2 days		7 days		2 (25%) days		7 (25%) days	
	Fresh 2	Aged 2	Fresh 7	Aged 7[b]	Fresh 2	Aged 2	Fresh 7	Aged 7
Peat IDs in the average[c]	PEAT013, PEAT014, PEAT019		PEAT020, PEAT022		PEAT008, PEAT009		PEAT005, PEAT006	
Nitric Acid (HNO_3)	0.40 ± 0.19	0.31 ± 0.15	0.29 ± 0.22	0.28 ± 0.10	0.18 ± 0.033	0.39 ± 0.17	0.32 ± 0.25	0.23 ± 0.0055
Ammonia (NH_3)	16.64 ± 8.41	6.39 ± 3.76	27.73 ± 11.16	5.13 ± 0.80	28.03 ± 2.90	4.76 ± 0.52	na[f]	1.39 ± 0.62
Water-Soluble Sodium (Na^+)	0.047 ± 0.035	0.13 ± 0.15	0.047 ± 0.036	0.053 ± 0.022	0.015 ± 0.00033	0.033 ± 0.00033	0.030 ± 0.0058	0.032 ± 0.0048
Water-Soluble Potassium (K^+)	0.042 ± 0.068	na[d]	0.035 ± 0.010	na[d]	0.010 ± 0.015	na[d]	0.029 ± 0.0042	na[d]
Chloride (Cl^-)	0.21 ± 0.050	0.25 ± 0.19	0.29 ± 0.029	0.11 ± 0.0042	0.14 ± 0.035	0.18 ± 0.10	0.14 ± 0.041	0.087 ± 0.0049
Nitrite (NO_2^-)	0.15 ± 0.25	0.0015 ± 0.0019	0.00 ± 0.00040	0.0014 ± 0.00094	0.053 ± 0.071	0.011 ± 0.015	0.00044 ± 0.00062	0.0012 ± 0.00037
Nitrate (NO_3^-)	0.20 ± 0.16	1.45 ± 0.79	0.17 ± 0.053	8.19 ± 5.96	0.16 ± 0.12	0.87 ± 0.15	0.040 ± 0.000070	1.10 ± 0.18
Sulfate ($SO_4^=$)	0.46 ± 0.38	0.35 ± 0.16	0.26 ± 0.24	0.64 ± 0.23	0.89 ± 0.97	1.60 ± 1.33	0.22 ± 0.013	1.29 ± 0.13
Ammonium (NH_4^+)	0.11 ± 0.19	0.66 ± 0.78	0.0028 ± 0.00085	4.30 ± 0.098	0.00070 ± 0.00099	0.052 ± 0.074	0.00046 ± 0.000031	1.0080 ± 0.048
OC1 (140°C)	14.58 ± 4.92	10.33 ± 4.49	9.28 ± 4.049	3.76 ± 1.77	9.54 ± 2.50	7.48 ± 3.12	13.15 ± 3.56	10.087 ± 1.63
OC2 (280°C)	21.37 ± 0.70	17.98 ± 1.13	17.28 ± 3.42	9.68 ± 3.57	21.66 ± 2.045	19.50 ± 0.85	20.74 ± 2.34	19.76 ± 2.57
OC3 (480°C)	26.36 ± 5.88	24.57 ± 6.14	28.99 ± 14.35	18.47 ± 5.013	25.30 ± 7.61	24.97 ± 0.95	20.38 ± 0.63	21.97 ± 1.65
OC4 (580°C)	7.70 ± 1.79	6.51 ± 1.99	8.0014 ± 4.44	8.56 ± 2.51	7.60 ± 4.045	7.76 ± 1.017	4.29 ± 0.0044	5.34 ± 2.10
Pyrolized Carbon (OP)	7.40 ± 1.69	10.66 ± 4.45	7.35 ± 2.14	6.68 ± 3.39	7.61 ± 1.80	10.45 ± 1.14	8.81 ± 0.79	10.73 ± 0.53
Organic Carbon (OC)	77.41 ± 6.13	70.047 ± 8.98	70.91 ± 20.30	47.16 ± 11.23	71.71 ± 9.40	70.16 ± 5.033	67.37 ± 4.48	67.88 ± 5.22
EC1 (580°C)	6.050 ± 1.50	9.94 ± 2.92	5.24 ± 1.038	7.11 ± 3.90	7.61 ± 2.43	9.58 ± 1.36	6.44 ± 0.099	8.98 ± 1.36
EC2 (740°C)	3.43 ± 3.013	2.93 ± 2.14	5.70 ± 1.85	1.63 ± 1.99	3.51 ± 2.51	2.94 ± 2.34	4.057 ± 0.60	3.28 ± 0.88
EC3 (840°C)	0.00 ± 0.00020	0.00 ± 0.00021	0.00 ± 0.00029	0.00 ± 0.00022	0.00 ± 0.00014	0.00 ± 0.00015	0.00 ± 0.00011	0.00 ± 0.00010
Elemental Carbon (EC)	2.082 ± 1.079	2.21 ± 0.99	3.59 ± 0.75	2.047 ± 2.51	3.51 ± 1.72	2.076 ± 0.16	1.69 ± 0.29	1.53 ± 0.057
Total Carbon (TC)	79.49 ± 7.072	72.26 ± 8.88	74.50 ± 21.052	49.20 ± 13.74	75.23 ± 11.12	72.24 ± 4.88	69.06 ± 4.77	69.41 ± 5.16
Water-Soluble OC (WSOC)	29.32 ± 9.03	28.35 ± 3.81	31.58 ± 11.22	25.77 ± 4.05	19.53 ± 4.67	22.71 ± 4.43	16.33 ± 1.17	23.15 ± 1.45
Formate ($CH_2O_2^-$)	0.093 ± 0.029	0.21 ± 0.049	0.069 ± 0.018	0.25 ± 0.11	0.11 ± 0.097	0.20 ± 0.13	0.022 ± 0.0044	0.15 ± 0.0065
Acetate ($C_2H_4O_2^-$)	0.38 ± 0.15	0.64 ± 0.17	0.45 ± 0.24	0.34 ± 0.26	0.19 ± 0.15	0.047 ± 0.011	0.056 ± 0.010	0.26 ± 0.024
Oxalate ($C_2H_2O_4^=$)	0.039 ± 0.028	0.86 ± 0.16	0.043 ± 0.061	3.26 ± 0.52	0.050 ± 0.070	0.58 ± 0.26	0.00 ± 0.02	1.12 ± 0.19
Propionate ($C_3H_5O_2^-$)	0.0072 ± 0.010	0.024 ± 0.034	0.00 ± 0.00020	0.034 ± 0.048	0.00 ± 0.000099	0.00 ± 0.00010	0.00 ± 0.000077	0.00 ± 0.000071
Levoglucosan ($C_6H_{10}O_5$)	17.87 ± 8.03	16.99 ± 3.32	9.78 ± 1.15	4.87 ± 2.89	3.15 ± 0.0092	2.78 ± 0.041	3.12 ± 0.24	1.49 ± 0.50
Mannosan ($C_6H_{10}O_5$)	3.46 ± 1.25	3.53 ± 1.26	2.73 ± 0.40	0.95 ± 0.34	0.00 ± 0.00022	0.00 ± 0.00023	0.00 ± 0.00017	0.00 ± 0.00016
Galactose/Maltitol ($C_6H_{12}O_6$/$C_{12}H_{24}O_{11}$)	0.00 ± 0.00015	0.00 ± 0.00016	0.00 ± 0.00022	0.00 ± 0.00017	0.00 ± 0.00011	0.00 ± 0.00012	0.00 ± 0.00087	0.00 ± 0.000079
Glycerol ($C_3H_8O_3$)	0.23 ± 0.33	0.20 ± 0.28	0.98 ± 1.39	0.12 ± 0.17	0.00 ± 0.0000050	0.00 ± 0.0000021	0.00 ± 0.0000015	0.00 ± 0.0000014
Mannitol ($C_6H_{14}O_6$)	0.00 ± 0.000055	0.10 ± 0.15	0.00 ± 0.000080	0.00 ± 0.000061	0.00 ± 0.000039	0.00 ± 0.000042	0.00 ± 0.000056	0.00 ± 0.000028
Aluminum (Al)	0.026 ± 0.24	0.063 ± 0.28	0.029 ± 0.13	0.0098 ± 0.0046	0.026 ± 0.059	0.069 ± 0.97	0.12 ± 1.34	0.080 ± 0.61
Silicon (Si)	0.0077 ± 0.12	0.0069 ± 0.098	0.0012 ± 0.017	0.63 ± 0.00060	0.00 ± 0.00030	0.021 ± 0.22	0.00 ± 0.0021	0.021 ± 0.067
Phosphorous (P)	0.00 ± 0.000084	0.00 ± 0.00011	0.00 ± 0.00012	0.00 ± 0.00011	0.00 ± 0.000060	0.00 ± 0.000064	0.00 ± 0.000048	0.00 ± 0.000044

Table 1 (cont'd)

Sulfur (S)	0.031 ± 0.054	0.062 ± 0.087	0.0099 ± 0.014	0.34 ± 0.00013	0.19 ± 0.056	0.37 ± 0.24	0.17 ± 0.037	0.74 ± 0.047
Chlorine (Cl)	0.12 ± 0.068	0.087 ± 0.030	0.14 ± 0.049	0.019 ± 0.000040	0.12 ± 0.0064	0.067 ± 0.024	0.14 ± 0.022	0.056 ± 0.00047
Potassium (K)	0.046 ± 0.016	0.16 ± 0.15	0.052 ± 0.046	0.47 ± 0.00022	0.0092 ± 0.012	0.057 ± 0.035	0.0046 ± 0.00044	0.12 ± 0.10
Calcium (Ca)	0.032 ± 0.032	0.032 ± 0.045	0.035 ± 0.049	0.00 ± 0.00057	0.0040 ± 0.0056	0.00 ± 0.00034	0.00 ± 0.00025	0.00 ± 0.00023
Scandium (Sc)	0.00 ± 0.0020	0.00 ± 0.0025	0.00 ± 0.0029	0.00 ± 0.0026	0.00 ± 0.0014	0.00 ± 0.0015	0.022 ± 0.031	0.00 ± 0.0010
Titanium (Ti)	0.00 ± 0.000071	0.00 ± 0.000091	0.0055 ± 0.0078	0.051 ± 0.000093	0.0036 ± 0.0050	0.00 ± 0.000054	0.0086 ± 0.012	0.00 ± 0.000037
Vanadium (V)	0.00 ± 0.000013	0.00 ± 0.000017	0.00 ± 0.000019	0.00 ± 0.000017	0.00 ± 0.000094	0.00 ± 0.000010	0.00 ± 0.0000075	0.00 ± 0.0000069
Chromium (Cr)	0.00051 ± 0.00089	0.00028 ± 0.00040	0.00 ± 0.000065	0.00 ± 0.000057	0.00 ± 0.000032	0.00 ± 0.000034	0.00034 ± 0.00048	0.00 ± 0.000023
Manganese (Mn)	0.0015 ± 0.0014	0.00069 ± 0.00098	0.0016 ± 0.0023	0.0011 ± 0.00020	0.0013 ± 0.0012	0.00033 ± 0.00047	0.00057 ± 0.00080	0.0016 ± 0.0018
Iron (Fe)	0.036 ± 0.014	0.10 ± 0.095	0.049 ± 0.048	0.029 ± 0.00035	0.00 ± 0.00019	0.047 ± 0.040	0.024 ± 0.012	0.065 ± 0.0091
Cobalt (Co)	0.00 ± 0.0000088	0.00 ± 0.000011	0.00 ± 0.000013	0.00013 ± 0.000011	0.00 ± 0.0000063	0.00021 ± 0.00030	0.00020 ± 0.00028	0.00 ± 0.0000046
Nickel (Ni)	0.00028 ± 0.00049	0.00 ± 0.000028	0.00075 ± 0.0011	0.00 ± 0.000028	0.00045 ± 0.00064	0.00 ± 0.000017	0.00069 ± 0.00097	0.00043 ± 0.00026
Copper (Cu)	0.028 ± 0.047	0.027 ± 0.034	0.0098 ± 0.0028	0.15 ± 0.00018	0.00 ± 0.000098	0.0035 ± 0.0049	0.0019 ± 0.0000053	0.069 ± 0.090
Zinc (Zn)	0.026 ± 0.036	0.027 ± 0.031	0.0026 ± 0.0020	0.011 ± 0.000097	0.0013 ± 0.0015	0.0023 ± 0.0032	0.00041 ± 0.000028	0.0046 ± 0.00037
Arsenic (As)	0.0006 ± 0.00078	0.00 ± 0.000045	0.00 ± 0.000052	0.00067 ± 0.000045	0.00 ± 0.000025	0.00 ± 0.000027	0.000062 ± 0.000087	0.00034 ± 0.00048
Selenium (Se)	0.00016 ± 0.00028	0.0064 ± 0.0017	0.0022 ± 0.0032	0.00 ± 0.000080	0.0017 ± 0.00092	0.00 ± 0.000047	0.00034 ± 0.00048	0.0034 ± 0.0017
Bromine (Br)	0.0017 ± 0.0018	0.0031 ± 0.0044	0.0079 ± 0.00064	0.0020 ± 0.000023	0.020 ± 0.00098	0.0077 ± 0.010	0.024 ± 0.0043	0.019 ± 0.0012
Rubidium (Rb)	0.00 ± 0.000022	0.0035 ± 0.0048	0.0057 ± 0.0059	0.0026 ± 0.000028	0.00011 ± 0.00016	0.00095 ± 0.0013	0.00 ± 0.000013	0.00066 ± 0.00047
Strontium (Sr)	0.0017 ± 0.00036	0.0076 ± 0.0084	0.0068 ± 0.0014	0.0028 ± 0.000028	0.0023 ± 0.00057	0.0038 ± 0.0013	0.0018 ± 0.00075	0.0046 ± 0.0025
Yttrium (Y)	0.0013 ± 0.0014	0.0037 ± 0.0013	0.0057 ± 0.0041	0.0054 ± 0.000028	0.0014 ± 0.00029	0.0012 ± 0.0018	0.00085 ± 0.000067	0.0022 ± 0.0032
Zirconium (Zr)	0.0027 ± 0.0028	0.0047 ± 0.0014	0.0025 ± 0.0027	0.011 ± 0.00011	0.0016 ± 0.0023	0.0003 ± 0.00089	0.00074 ± 0.0010	0.0013 ± 0.00079
Niobium (Nb)	0.00 ± 0.000040	0.00092 ± 0.00090	0.00027 ± 0.00039	0.00 ± 0.000051	0.0016 ± 0.0023	0.00082 ± 0.0012	0.00042 ± 0.00060	0.00 ± 0.000021
Molybdenum (Mo)	0.0012 ± 0.0019	0.0044 ± 0.0062	0.0020 ± 0.00084	0.00 ± 0.00011	0.00 ± 0.000060	0.00063 ± 0.00089	0.0025 ± 0.00092	0.00 ± 0.000044
Silver (Ag)	0.00 ± 0.00011	0.00 ± 0.00014	0.00 ± 0.00016	0.00 ± 0.00014	0.0010 ± 0.0014	0.00 ± 0.000081	0.00 ± 0.000060	0.00 ± 0.000055
Cadmium (Cd)	0.00 ± 0.00015	0.00 ± 0.00019	0.00 ± 0.00022	0.00 ± 0.00019	0.0034 ± 0.0049	0.00 ± 0.00011	0.0029 ± 0.00093	0.0020 ± 0.0029
Indium (In)	0.00082 ± 0.0013	0.0011 ± 0.0016	0.00069 ± 0.00097	0.00 ± 0.00013	0.00068 ± 0.00096	0.0025 ± 0.0036	0.0021 ± 0.0030	0.0018 ± 0.0026
Tin (Sn)	0.0045 ± 0.0078	0.014 ± 0.020	0.0067 ± 0.0025	0.00 ± 0.00024	0.0037 ± 0.00047	0.0034 ± 0.0048	0.0028 ± 0.0025	0.0074 ± 0.00049
Antimony (Sb)	0.0065 ± 0.011	0.015 ± 0.021	0.00 ± 0.00041	0.00 ± 0.00036	0.00 ± 0.00020	0.0072 ± 0.010	0.0020 ± 0.0029	0.00 ± 0.00015
Cesium (Cs)	0.0097 ± 0.0095	0.022 ± 0.031	0.010 ± 0.014	0.058 ± 0.0010	0.00 ± 0.00056	0.00 ± 0.00060	0.00 ± 0.00044	0.00 ± 0.00041
Barium (Ba)	0.00 ± 0.00059	0.00 ± 0.00077	0.00 ± 0.00086	0.00 ± 0.00089	0.00 ± 0.00042	0.00 ± 0.00046	0.00 ± 0.00034	0.00 ± 0.00031
Lanthanum (La)	0.015 ± 0.026	0.065 ± 0.025	0.055 ± 0.0026	0.00 ± 0.0015	0.042 ± 0.044	0.0053 ± 0.0075	0.019 ± 0.028	0.036 ± 0.021
Wolfram (W)	0.0034 ± 0.0059	0.0082 ± 0.0061	0.00 ± 0.00033	0.00 ± 0.00029	0.0037 ± 0.0018	0.0034 ± 0.0049	0.0019 ± 0.0028	0.00 ± 0.00012
Gold (Au)	0.00 ± 0.000066	0.0032 ± 0.0045	0.00 ± 0.000098	0.00 ± 0.000085	0.00062 ± 0.00088	0.00 ± 0.000051	0.00022 ± 0.00031	0.0012 ± 0.0017
Mercury (Hg)	0.00034 ± 0.00059	0.0014 ± 0.0020	0.00 ± 0.000052	0.00 ± 0.000045	0.00020 ± 0.00028	0.0014 ± 0.0020	0.00 ± 0.000020	0.00024 ± 0.00033
Lead (Pb)	0.00 ± 0.000066	0.0010 ± 0.0015	0.00 ± 0.000098	0.0036 ± 0.000085	0.0015 ± 0.0021	0.0014 ± 0.000962	0.00076 ± 0.0011	0.0012 ± 0.0017
Uranium (U)	0.0050 ± 0.0044	0.0028 ± 0.0027	0.0011 ± 0.0015	0.0035 ± 0.00015	0.0034 ± 0.0044	0.00 ± 0.000092	0.0026 ± 0.0037	0.00 ± 0.000062

https://doi.org/10.5194/amt-2019-198
Preprint. Discussion started: 29 May 2019

Table 1 (cont'd)

	Average ± Standard Deviation of Percent $PM_{2.5}$ Mass							
	Subtropical				Tropical			
	Everglades National Park, Florida				Borneo, Malaysia			
Aging Time	2 days		7 days		2 days		7 days	
	Fresh 2	Aged 2	Fresh 7	Aged 7	Fresh 2	Aged 2	Fresh 7	Aged 7
Peat IDs in the average[c]	PEAT010, PEAT011, PEAT012, PEAT015		PEAT016, PEAT017, PEAT018		PEAT036, PEAT038		PEAT039, PEAT041	
Nitric Acid (HNO_3)	0.38 ± 0.13	0.47 ± 0.37	0.28 ± 0.042	0.25 ± 0.13	0.20 ± 0.0080	0.26 ± 0.040	0.23 ± 0.18	0.17 ± 0.026
Ammonia (NH_3)	51.12 ± 27.44	14.37 ± 5.54	63.89 ± 25.088	4.79 ± 0.60	20.34 ± 0.0030	9.67 ± 2.25	25.50 ± 1.98	4.88 ± 1.76
Water-Soluble Sodium (Na^+)	0.047 ± 0.018	0.056 ± 0.016	0.030 ± 0.017	0.022 ± 0.0063	0.017 ± 0.0090	0.033 ± 0.023	0.018 ± 0.011	0.032 ± 0.017
Water-Soluble Potassium (K^+)	1.11 ± 2.15	na[d]	0.025 ± 0.017	na[d]	0.031 ± 0.028	na[d]	0.048 ± 0.035	na[d]
Chloride (Cl^-)	0.26 ± 0.072	0.21 ± 0.12	0.22 ± 0.018	0.086 ± 0.024	0.11 ± 0.024	0.10 ± 0.026	0.16 ± 0.073	0.10 ± 0.00025
Nitrite (NO_2^-)	0.058 ± 0.098	0.0020 ± 0.0031	0.00085 ± 0.0015	0.0023 ± 0.00072	0.00 ± 0.00025	0.00098 ± 0.0014	0.00 ± 0.00030	0.015 ± 0.019
Nitrate (NO_3^-)	0.27 ± 0.26	2.64 ± 0.76	0.14 ± 0.097	7.76 ± 1.029	0.087 ± 0.046	0.91 ± 0.22	0.13 ± 0.12	4.69 ± 1.34
Sulfate ($SO_4^=$)	1.40 ± 1.89	1.33 ± 0.69	0.34 ± 0.022	1.99 ± 0.28	0.17 ± 0.024	0.56 ± 0.18	0.13 ± 0.062	1.96 ± 0.071
Ammonium (NH_4^+)	0.0013 ± 0.0015	0.37 ± 0.60	0.0036 ± 0.00092	4.55 ± 0.57	0.0017 ± 0.0011	0.83 ± 0.086	0.0027 ± 0.00048	4.74 ± 0.77
OC1 (140°C)	11.40 ± 1.25	7.017 ± 3.95	18.049 ± 2.22	4.012 ± 0.89	16.033 ± 2.088	6.37 ± 3.36	15.20 ± 1.21	5.83 ± 3.45
OC2 (280°C)	23.86 ± 6.033	16.25 ± 3.60	24.53 ± 3.41	12.12 ± 0.86	22.44 ± 1.91	18.78 ± 4.51	23.41 ± 0.25	12.14 ± 2.71
OC3 (480°C)	23.70 ± 7.73	21.13 ± 3.73	23.33 ± 2.32	17.83 ± 3.95	25.52 ± 2.55	28.64 ± 4.52	26.24 ± 1.16	20.82 ± 3.30
OC4 (580°C)	9.010 ± 3.51	8.53 ± 2.94	6.15 ± 0.95	5.65 ± 1.23	4.37 ± 0.18	8.32 ± 1.099	5.56 ± 1.40	5.59 ± 0.82
Pyrolized Carbon (OP)	10.73 ± 2.31	9.89 ± 3.86	13.036 ± 1.020	12.30 ± 1.22	10.74 ± 0.66	12.56 ± 4.73	10.35 ± 0.11	13.15 ± 2.69
Organic Carbon (OC)	78.69 ± 18.69	62.82 ± 14.029	85.086 ± 5.65	51.90 ± 3.86	79.10 ± 3.21	74.66 ± 18.22	80.76 ± 0.99	57.53 ± 11.32
EC1 (580°C)	8.59 ± 4.065	8.56 ± 2.77	7.53 ± 1.22	11.035 ± 1.98	6.43 ± 0.48	8.57 ± 3.59	6.85 ± 0.21	9.13 ± 0.94
EC2 (740°C)	6.54 ± 2.76	3.42 ± 3.41	7.59 ± 1.66	3.35 ± 2.14	5.12 ± 0.25	6.18 ± 1.64	5.14 ± 0.16	4.69 ± 0.81
EC3 (840°C)	0.00 ± 0.00029	0.00 ± 0.00026	0.00 ± 0.00027	0.00 ± 0.00016	0.00 ± 0.00017	0.00 ± 0.00020	0.00 ± 0.00020	0.00 ± 0.00018
Elemental Carbon (EC)	4.40 ± 1.51	2.084 ± 0.52	2.084 ± 1.81	2.092 ± 1.11	0.82 ± 0.074	2.19 ± 0.50	1.63 ± 0.16	0.67 ± 0.94
Total Carbon (TC)	83.090 ± 19.45	64.90 ± 14.48	87.17 ± 7.38	54.00 ± 4.57	79.92 ± 3.29	76.86 ± 18.72	82.39 ± 1.14	58.20 ± 10.38
Water-Soluble OC (WSOC)	31.71 ± 8.36	28.89 ± 4.08	34.33 ± 4.82	23.28 ± 2.80	14.62 ± 0.92	22.88 ± 2.33	17.15 ± 2.80	22.90 ± 0.76
Formate ($CH_2O_2^-$)	0.14 ± 0.17	0.30 ± 0.052	0.054 ± 0.020	0.42 ± 0.23	0.10 ± 0.014	0.26 ± 0.049	0.13 ± 0.019	0.42 ± 0.10
Acetate ($C_2H_4O_2^-$)	0.33 ± 0.25	0.38 ± 0.063	0.22 ± 0.12	0.35 ± 0.13	0.29 ± 0.0081	0.59 ± 0.24	0.58 ± 0.075	0.56 ± 0.018
Oxalate ($C_2H_2O_4^=$)	0.11 ± 0.058	0.94 ± 0.22	0.082 ± 0.029	3.14 ± 0.56	0.26 ± 0.12	1.14 ± 0.21	0.43 ± 0.22	3.36 ± 0.28
Propionate ($C_3H_5O_2^-$)	0.0064 ± 0.013	0.00 ± 0.00018	0.018 ± 0.031	0.012 ± 0.020	0.045 ± 0.019	0.0095 ± 0.013	0.012 ± 0.017	0.066 ± 0.094
Levoglucosan ($C_6H_{10}O_5$)	1.08 ± 1.34	0.86 ± 1.073	2.22 ± 0.66	0.62 ± 0.81	2.52 ± 0.016	2.28 ± 0.99	4.38 ± 0.50	2.53 ± 0.19
Mannosan ($C_6H_{10}O_5$)	0.00 ± 0.00045	0.00 ± 0.00039	0.056 ± 0.097	0.24 ± 0.42	0.00 ± 0.00027	0.00 ± 0.00030	0.19 ± 0.26	0.082 ± 0.12
Galactose/Maltitol ($C_6H_{12}O_6$/$C_{12}H_{24}O_{11}$)	0.00 ± 0.00023	0.00 ± 0.00020	0.00 ± 0.00021	0.00 ± 0.00012	0.00 ± 0.00014	0.13 ± 0.18	0.00 ± 0.00017	0.00 ± 0.00014
Glycerol ($C_3H_8O_3$)	0.00 ± 0.0000041	0.00 ± 0.0000036	0.00 ± 0.0000038	0.00 ± 0.0000022	0.00 ± 0.0000025	0.00 ± 0.0000028	0.00 ± 0.0000030	0.00 ± 0.0000024
Mannitol ($C_6H_{14}O_6$)	0.00 ± 0.000083	0.00 ± 0.000072	0.00 ± 0.000075	0.00 ± 0.000043	0.011 ± 0.016	0.00 ± 0.000055	0.00 ± 0.000060	0.00 ± 0.000049
Aluminum (Al)	0.043 ± 0.86	0.070 ± 1.20	0.00024 ± 0.0041	0.00 ± 0.026[e]	0.033 ± 0.47	0.085 ± 0.030	0.045 ± 0.64	0.15 ± 0.030
Silicon (Si)	0.027 ± 0.52	0.26 ± 3.92	0.00 ± 0.00059	0.46 ± 0.31	0.012 ± 0.17	0.082 ± 0.0036	0.00 ± 0.00043	0.69 ± 0.0043
Phosphorous (P)	0.00 ± 0.00013	0.00 ± 0.00011	0.00 ± 0.00012	0.00 ± 0.000061	0.00 ± 0.000072	0.00 ± 0.000071	0.00 ± 0.000086	0.00 ± 0.000071

https://doi.org/10.5194/amt-2019-198
Preprint. Discussion started: 29 May 2019

Table 1 (cont'd)

Sulfur (S)	0.39 ± 0.23	0.59 ± 0.27	0.42 ± 0.066	1.12 ± 0.094	0.11 ± 0.12	0.39 ± 0.00013	0.029 ± 0.0022	0.83 ± 0.00026
Chlorine (Cl)	0.21 ± 0.088	0.065 ± 0.029	0.24 ± 0.024	0.038 ± 0.011	0.074 ± 0.0012	0.067 ± 0.000035	0.085 ± 0.0038	0.047 ± 0.000030
Potassium (K)	0.034 ± 0.015	0.51 ± 0.37	0.018 ± 0.014	0.22 ± 0.052	0.051 ± 0.049	0.084 ± 0.00010	0.028 ± 0.017	0.017 ± 0.00010
Calcium (Ca)	0.00 ± 0.00067	0.0081 ± 0.016	0.00 ± 0.00061	0.010 ± 0.014	0.0058 ± 0.0082	0.00 ± 0.00037	0.00 ± 0.00046	0.023 ± 0.00038
Scandium (Sc)	0.00 ± 0.0030	0.00 ± 0.0026	0.00 ± 0.0027	0.00 ± 0.0014	0.00 ± 0.0017	0.00 ± 0.0017	0.00 ± 0.0020	0.00 ± 0.0017
Titanium (Ti)	0.0061 ± 0.0079	0.017 ± 0.035	0.00 ± 0.000098	0.00 ± 0.000051	0.0073 ± 0.010	0.00 ± 0.000059	0.0066 ± 0.0094	0.00 ± 0.000059
Vanadium (V)	0.0010 ± 0.0020	0.00 ± 0.000017	0.00 ± 0.000018	0.0065 ± 0.0092	0.00 ± 0.000011	0.00 ± 0.000011	0.00 ± 0.000014	0.00 ± 0.000011
Chromium (Cr)	0.00 ± 0.000066	0.00056 ± 0.0011	0.00 ± 0.000061	0.00016 ± 0.00023	0.00 ± 0.000038	0.00 ± 0.000037	0.0026 ± 0.0037	0.00 ± 0.000037
Manganese (Mn)	0.0032 ± 0.0064	0.0051 ± 0.0050	0.0017 ± 0.0015	0.0034 ± 0.0043	0.0055 ± 0.0026	0.0075 ± 0.00013	0.0088 ± 0.00010	0.0046 ± 0.00013
Iron (Fe)	0.023 ± 0.021	0.065 ± 0.034	0.020 ± 0.016	0.091 ± 0.096	0.074 ± 0.0078	0.074 ± 0.00023	0.045 ± 0.020	0.043 ± 0.00023
Cobalt (Co)	0.000055 ± 0.00011	0.000045 ± 0.000090	0.00024 ± 0.00041	0.00 ± 0.0000064	0.00 ± 0.0000075	0.00061 ± 0.0000074	0.00 ± 0.0000090	0.000087 ± 0.0000074
Nickel (Ni)	0.00026 ± 0.00042	0.00 ± 0.000029	0.00 ± 0.000031	0.00038 ± 0.00054	0.00064 ± 0.00091	0.00 ± 0.000019	0.0034 ± 0.0014	0.00 ± 0.000019
Copper (Cu)	0.010 ± 0.0080	0.21 ± 0.23	0.0033 ± 0.0036	0.021 ± 0.0024	0.0054 ± 0.0042	0.0075 ± 0.00012	0.0091 ± 0.0013	0.0017 ± 0.00012
Zinc (Zn)	0.0039 ± 0.0011	0.0091 ± 0.0039	0.0021 ± 0.0019	0.023 ± 0.027	0.0043 ± 0.0037	0.00 ± 0.000063	0.0034 ± 0.0018	0.00 ± 0.000063
Arsenic (As)	0.00059 ± 0.00069	0.0013 ± 0.0020	0.00 ± 0.000049	0.00 ± 0.000025	0.00 ± 0.000030	0.00 ± 0.000030	0.00 ± 0.000036	0.0028 ± 0.000030
Selenium (Se)	0.0011 ± 0.0014	0.0023 ± 0.0018	0.0037 ± 0.0025	0.00016 ± 0.00023	0.0019 ± 0.0010	0.00 ± 0.000052	0.00086 ± 0.0012	0.00 ± 0.000052
Bromine (Br)	0.030 ± 0.015	0.0090 ± 0.0049	0.022 ± 0.0072	0.0088 ± 0.0036	0.011 ± 0.0015	0.012 ± 0.000015	0.012 ± 0.0026	0.0044 ± 0.000015
Rubidium (Rb)	0.00038 ± 0.00077	0.0015 ± 0.0014	0.0015 ± 0.0026	0.00 ± 0.000016	0.00039 ± 0.00056	0.00035 ± 0.000019	0.00 ± 0.000023	0.0017 ± 0.000019
Strontium (Sr)	0.0051 ± 0.0012	0.0044 ± 0.0023	0.0055 ± 0.0063	0.0033 ± 0.0022	0.0028 ± 0.00026	0.0021 ± 0.000019	0.0070 ± 0.00099	0.0029 ± 0.000019
Yttrium (Y)	0.0043 ± 0.0051	0.0021 ± 0.0034	0.0014 ± 0.00060	0.00 ± 0.0000016	0.0018 ± 0.0023	0.0032 ± 0.000019	0.0018 ± 0.0016	0.0027 ± 0.000019
Zirconium (Zr)	0.0041 ± 0.0038	0.0049 ± 0.0066	0.0040 ± 0.0069	0.0051 ± 0.0039	0.0048 ± 0.00038	0.0016 ± 0.000071	0.00052 ± 0.00074	0.00 ± 0.000071
Niobium (Nb)	0.0016 ± 0.0022	0.00080 ± 0.0013	0.0019 ± 0.0026	0.00 ± 0.000029	0.00095 ± 0.0014	0.00 ± 0.000034	0.0021 ± 0.0030	0.00026 ± 0.000034
Molybdenum (Mo)	0.0022 ± 0.0021	0.0013 ± 0.0017	0.0012 ± 0.0022	0.00081 ± 0.0011	0.00071 ± 0.0010	0.00 ± 0.000071	0.0044 ± 0.00018	0.0032 ± 0.000071
Silver (Ag)	0.0014 ± 0.0029	0.00 ± 0.00014	0.00 ± 0.00015	0.00 ± 0.000076	0.0025 ± 0.0035	0.00 ± 0.000089	0.0026 ± 0.0037	0.00 ± 0.000089
Cadmium (Cd)	0.00 ± 0.00022	0.00 ± 0.00019	0.0075 ± 0.013	0.0095 ± 0.0060	0.00044 ± 0.00063	0.00 ± 0.00012	0.00 ± 0.00015	0.00 ± 0.00012
Indium (In)	0.0069 ± 0.0049	0.0023 ± 0.0046	0.0054 ± 0.0093	0.0012 ± 0.0017	0.0048 ± 0.0067	0.0013 ± 0.000085	0.00087 ± 0.0012	0.00 ± 0.000085
Tin (Sn)	0.0061 ± 0.0072	0.0058 ± 0.012	0.0061 ± 0.0058	0.0068 ± 0.0096	0.0022 ± 0.0031	0.013 ± 0.00016	0.0038 ± 0.0054	0.012 ± 0.00016
Antimony (Sb)	0.00028 ± 0.00056	0.00040 ± 0.00052	0.00033 ± 0.00057	0.00050 ± 0.00071	0.00 ± 0.00024	0.0039 ± 0.00023	0.011 ± 0.0097	0.00 ± 0.00023
Cesium (Cs)	0.000088 ± 0.00018	0.028 ± 0.037	0.037 ± 0.064	0.00 ± 0.00057	0.028 ± 0.031	0.020 ± 0.00066	0.0077 ± 0.011	0.00 ± 0.00066
Barium (Ba)	0.00 ± 0.00088	0.00 ± 0.00085	0.00 ± 0.00081	0.00 ± 0.00044	0.00 ± 0.00050	0.00 ± 0.00050	0.00 ± 0.00060	0.00 ± 0.00050
Lanthanum (La)	0.054 ± 0.039	0.033 ± 0.039	0.036 ± 0.039	0.0049 ± 0.0070	0.041 ± 0.058	0.00 ± 0.00097	0.018 ± 0.025	0.080 ± 0.00097
Wolfram (W)	0.010 ± 0.012	0.0030 ± 0.0051	0.0080 ± 0.014	0.00 ± 0.00016	0.00 ± 0.00019	0.0058 ± 0.00019	0.00 ± 0.00023	0.00 ± 0.00019
Gold (Au)	0.0012 ± 0.0013	0.00082 ± 0.0016	0.0046 ± 0.0045	0.00033 ± 0.00047	0.00051 ± 0.00072	0.00 ± 0.000056	0.00041 ± 0.00058	0.00 ± 0.000056
Mercury (Hg)	0.00035 ± 0.00070	0.00091 ± 0.0015	0.00 ± 0.000049	0.00 ± 0.000025	0.00 ± 0.000030	0.00 ± 0.000030	0.00041 ± 0.00058	0.000087± 0.000030
Lead (Pb)	0.0017 ± 0.0035	0.0012 ± 0.0024	0.0018 ± 0.0031	0.0028 ± 0.0026	0.0031 ± 0.0044	0.00052 ± 0.000056	0.0016 ± 0.0022	0.00 ± 0.000056
Uranium (U)	0.0027 ± 0.0031	0.0023 ± 0.0026	0.0044 ± 0.0077	0.0017 ± 0.0023	0.00 ± 0.00010	0.0033 ± 0.00010	0.0057 ± 0.00076	0.0062 ± 0.00010

[a]Analytical uncertainties are used for species below the minimum detection limit, mostly for carbohydrate species and elements with an average concentration of 0.00
[b]Only one sample was analyzed for elements by x-ray fluorescence with abundance and measurement uncertainty
[c]Peat ID code, detailed operation parameters are reported in Watson et al. (2019)

https://doi.org/10.5194/amt-2019-198
Preprint. Discussion started: 29 May 2019

Atmospheric Measurement Techniques Discussions
Open Access

[d]Data not available; water-soluble K^+ data were contaminated for aged samples due to the use of potassium iodide denuder downstream of the oxidation flow reactor

[e]WSOC measures from Peat sample ID PEAT028 was invalidated due to a crack in the test tube. Therefore, only two measurements are used to calculate the average and standard deviation.

[f]Data not available due to the invalidated citric acid impregnated filter sample

Table 2. Equivalence measures[a] for comparison of $PM_{2.5}$ peat source profiles. Highlighted *P*-values <0.05 indicate significant differences at the 95% confidence level.

All Fresh (Profile #1) vs. All Aged (Profile #2) by Biome (group comparison of fresh and aged samples)

				Percent Distribution				Correlation	
Peat region[b]	Peats Included	n1[c]	n2[c]	< 1 σ	1 - 2 σ	2 - 3 σ	> 3 σ	Coefficient	*P*-value[d]
Boreal	Russia + Siberia	12	12	93.60%	5.60%	0.80%	0.00%	0.995	0.00012
Boreal + Temperate	Russia + Siberia + Alaska	17	17	95.20%	4.80%	0.00%	0.00%	0.996	0.00010
Temperate	Alaska	5	5	96.00%	4.00%	0.00%	0.00%	0.997	0.00008
Subtropical	Florida	11	11	92.86%	7.14%	0.00%	0.00%	0.985	0.00007
Subtropical + Temperate	Alaska + Florida	16	16	94.44%	5.56%	0.00%	0.00%	0.992	0.00004
Tropical	Malaysia	4	4	78.57%	18.25%	1.59%	1.59%	0.994	0.00195
Subtropical + Tropical	Florida + Malaysia	15	15	93.65%	6.35%	0.00%	0.00%	0.990	0.00009

Fresh 2 vs. Aged 2 by Biome (paired comparison for 2-day aging)

				Percent Distribution				Correlation	
Peat region[b]	Peats Included	n1[c]	n2[c]	< 1 σ	1 - 2 σ	2 - 3 σ	> 3 σ	Coefficient	*P*-value[d]
Boreal	Russia + Siberia	6	6	94.40%	3.20%	2.40%	0.00%	0.997	0.00088
Boreal + Temperate	Russia + Siberia + Alaska	9	9	95.20%	4.00%	0.80%	0.00%	0.997	0.00237
Temperate	Alaska	3	3	86.40%	11.20%	0.80%	1.60%	0.997	0.02474
Subtropical	Florida	6	6	92.86%	6.35%	0.79%	0.00%	0.992	0.00001
Subtropical + Temperate	Alaska + Florida	9	9	96.83%	2.38%	0.00%	0.79%	0.996	0.00006
Tropical	Malaysia	2	2	80.00%	5.33%	5.33%	9.33%	0.996	0.95960
Subtropical + Tropical	Florida + Malaysia	8	8	96.83%	2.38%	0.79%	0.00%	0.995	0.00007

Fresh 7 vs. Aged 7 by Biome (paired comparison for 7-day aging)

				Percent Distribution				Correlation	
Peat region[b]	Peats Included	n1[c]	n2[c]	< 1 σ	1 - 2 σ	2 - 3 σ	> 3 σ	Coefficient	*P*-value[d]
Boreal	Russia + Siberia	6	6	76.00%	20.80%	1.60%	1.60%	0.992	0.00007
Boreal + Temperate	Russia + Siberia + Alaska	8	8	76.80%	20.00%	0.80%	2.40%	0.993	0.00003
Temperate	Alaska	2	2	64.86%	25.68%	2.70%	6.76%	0.993	0.00000
Subtropical	Florida	5	5	73.02%	23.81%	2.38%	0.79%	0.974	0.00023
Subtropical + Temperate	Alaska + Florida	7	7	75.40%	23.02%	1.59%	0.00%	0.984	0.00004
Tropical	Malaysia	2	2	41.33%	21.33%	24.00%	13.33%	0.989	0.00017
Subtropical + Tropical	Florida + Malaysia	7	7	75.40%	21.43%	2.38%	0.79%	0.983	0.00012

Fresh 2 vs. Fresh 7 by Biome (comparison between different experimentsfor unaged fresh profiles)

				Percent Distribution				Correlation	
Peat region[b]	Peats Included	n1[c]	n2[c]	< 1 σ	1 - 2 σ	2 - 3 σ	> 3 σ	Coefficient	*P*-value[d]
Boreal	Russia + Siberia	6	6	97.62%	2.38%	0.00%	0.00%	0.999	0.00004
Boreal + Temperate	Russia + Siberia + Alaska	9	8	100.00%	0.00%	0.00%	0.00%	0.999	0.00148
Temperate	Alaska	3	2	91.27%	6.35%	0.79%	1.59%	0.996	0.12876
Subtropical	Florida	6	5	98.41%	1.59%	0.00%	0.00%	0.997	0.52344
Subtropical + Temperate	Alaska + Florida	9	7	100.00%	0.00%	0.00%	0.00%	0.998	0.93350
Tropical	Malaysia	2	2	81.10%	10.24%	3.15%	5.51%	0.999	0.00006
Subtropical + Tropical	Florida + Malaysia	8	7	100.00%	0.00%	0.00%	0.00%	0.999	0.11445

Aged 2 vs. Aged 7 by Biome (comparison between different experiments for the 2- and 7-day aging times)

				Percent Distribution				Correlation	
Peat region[b]	Peats Included	n1[c]	n2[c]	< 1 σ	1 - 2 σ	2 - 3 σ	> 3 σ	Coefficient	*P*-value[d]
Boreal	Russia + Siberia	6	6	95.20%	3.20%	1.60%	0.00%	0.997	0.00018
Boreal + Temperate	Russia + Siberia + Alaska	9	8	94.40%	3.20%	1.60%	0.80%	0.998	0.00002
Temperate	Alaska	3	2	66.22%	27.03%	5.41%	1.35%	0.996	0.00000
Subtropical	Florida	6	5	93.65%	6.35%	0.00%	0.00%	0.998	0.00194
Subtropical + Temperate	Alaska + Florida	9	7	98.41%	1.59%	0.00%	0.00%	0.998	0.00002
Tropical	Malaysia	2	2	81.33%	13.33%	1.33%	4.00%	0.997	0.00002
Subtropical + Tropical	Florida + Malaysia	8	7	96.03%	3.97%	0.00%	0.00%	0.998	0.00026

[a]For the *t*-test, a cutoff probability level of 5% is selected; if $P < 0.05$, there is a 95% probability that the two profiles are different. For correlations, $r > 0.8$ suggests similar profiles, $0.5 < r < 0.8$ indicates a moderate similarity, and $r < 0.5$ denotes little or no similarity. The *R*/*U* ratio indicates the percentage of the >93 reported chemical abundances differ by more than an expected number of uncertainty intervals. The normal probability density function of 68%, 95.5%, and 99.7% for $\pm 1\sigma$, $\pm 2\sigma$, and $\pm 3\sigma$, respectively, is used to evaluate the *R*/*U* ratios. The two profiles are considered to be similar, within the uncertainties of the chemical abundances when 80% of the *R*/*U* ratios are within $\pm 3\sigma$, with $r > 0.8$ and $P > 0.05$. Species with *R*/*U* ratios $> 3\sigma$ are further examined as these may be markers that further allow source contributions to be distinguishes by receptor measurements. They may also reflect the sampling and analysis artifacts that are not representative of the larger population of source profiles.

[b]Unless otherwise noted, Boreal represents Russia and Siberia regions, Temperate represents northern Alaska region, Subtropical represents north and south Florida regions, and Tropical represents Island of Borneo, Malaysia region.

[c]n1 and n2 denote number of samples in comparison

[d]Student *t*-test *P*-values

https://doi.org/10.5194/amt-2019-198
Preprint. Discussion started: 29 May 2019

Atmospheric Measurement Techniques Discussions

Table 3. Organic carbon diagnostic ratios for different peat samples.

Peat Type	Atmospheric Aging time	OC/TC ± σ[a]	OM[b]/OC ± σ[a]	WSOC[c]/OC ± σ[a]	(Levoglucosan/2.25)[d]/OC ± σ[a]	(Oxalate/3.75)[e]/OC ± σ[a]	(Levoglucosan/2.25)[d]/WSOC ± σ[a]	(Oxalate/3.75)[e]/WSOC ± σ[a]
Odintsovo, Russia	Fresh 2	0.97 ± 0.11	1.7 ± 0.15	0.64 ± 0.075	0.27 ± 0.066	0.00047 ± 0.00029	0.42 ± 0.10	0.00073 ± 0.00045
	Aged 2	0.97 ± 0.30	2.1 ± 0.46	0.70 ± 0.17	0.24 ± 0.10	0.0057 ± 0.0017	0.35 ± 0.13	0.0082 ± 0.0019
	Fresh 7	0.97 ± 0.12	1.6 ± 0.14	0.59 ± 0.065	0.28 ± 0.030	0.0012 ± 0.001	0.48 ± 0.040	0.0021 ± 0.0017
	Aged 7	0.95 ± 0.16	2.2 ± 0.26	0.71 ± 0.18	0.21 ± 0.051	0.019 ± 0.0055	0.30 ± 0.089	0.026 ± 0.0090
Pskov, Siberia	Fresh 2	0.96 ± 0.12	1.3 ± 0.12	0.32 ± 0.039	0.04 ± 0.016	0.00023 ± 0.000050	0.12 ± 0.049	0.00069 ± 0.00015
	Aged 2	0.96 ± 0.26	1.4 ± 0.27	0.44 ± 0.13	0.027 ± 0.0066	0.0051 ± 0.0021	0.063 ± 0.017	0.012 ± 0.0050
	Fresh 7	0.99 ± 0.17	1.2 ± 0.14	0.40 ± 0.046	0.051 ± 0.013	0.00025 ± 0.000067	0.13 ± 0.055	0.00063 ± 0.00015
	Aged 7	0.96 ± 0.14	1.5 ± 0.18	0.56 ± 0.17	0.031 ± 0.0043	0.019 ± 0.0073	0.057 ± 0.018	0.035 ± 0.016
Northern Alaska, USA	Fresh 2	0.97 ± 0.12	1.3 ± 0.10	0.38 ± 0.12	0.10 ± 0.047	0.00013 ± 0.00010	0.27 ± 0.15	0.00035 ± 0.00028
	Aged 2	0.97 ± 0.17	1.4 ± 0.18	0.40 ± 0.075	0.11 ± 0.025	0.0033 ± 0.00073	0.27 ± 0.063	0.0080 ± 0.0018
	Fresh 7	0.95 ± 0.38	1.4 ± 0.39	0.45 ± 0.20	0.061 ± 0.019	0.00016 ± 0.00023	0.14 ± 0.052	0.00037 ± 0.00053
	Aged 7	0.96 ± 0.35	1.8 ± 0.44	0.55 ± 0.16	0.046 ± 0.029	0.018 ± 0.0053	0.084 ± 0.052	0.034 ± 0.0076
Putnam County Lakebed, Florida, USA	Fresh 2	0.95 ± 0.19	1.3 ± 0.18	0.27 ± 0.074	0.02 ± 0.0026	0.00019 ± 0.00026	0.072 ± 0.017	0.00068 ± 0.0010
	Aged 2	0.97 ± 0.10	1.4 ± 0.10	0.32 ± 0.067	0.018 ± 0.0013	0.0022 ± 0.0010	0.054 ± 0.011	0.0068 ± 0.0033
	Fresh 7	0.98 ± 0.094	1.5 ± 0.10	0.24 ± 0.024	0.021 ± 0.0021	na	0.085 ± 0.009	na
	Aged 7	0.98 ± 0.10	1.4 ± 0.11	0.34 ± 0.034	0.010 ± 0.0034	0.0044 ± 0.00082	0.029 ± 0.010	0.013 ± 0.0023
Everglades, Florida, USA	Fresh 2	0.95 ± 0.32	1.2 ± 0.28	0.40 ± 0.14	0.0061 ± 0.0077	0.00036 ± 0.00021	0.015 ± 0.019	0.00089 ± 0.00054
	Aged 2	0.97 ± 0.31	1.5 ± 0.33	0.46 ± 0.12	0.0061 ± 0.0077	0.0044 ± 0.00082	0.013 ± 0.017	0.0086 ± 0.0024
	Fresh 7	0.98 ± 0.11	1.1 ± 0.079	0.40 ± 0.063	0.012 ± 0.0035	0.00026 ± 0.000092	0.029 ± 0.009	0.00064 ± 0.00024
	Aged 7	0.96 ± 0.11	1.6 ± 0.12	0.45 ± 0.063	0.0053 ± 0.007	0.016 ± 0.0031	0.012 ± 0.016	0.036 ± 0.0078
Borneo, Malaysia	Fresh 2	0.99 ± 0.057	1.2 ± 0.051	0.18 ± 0.014	0.014 ± 0.00058	0.00087 ± 0.00042	0.077 ± 0.005	0.0047 ± 0.0023
	Aged 2	0.97 ± 0.33	1.3 ± 0.31	0.31 ± 0.081	0.014 ± 0.0067	0.0041 ± 0.0012	0.044 ± 0.020	0.013 ± 0.0028
	Fresh 7	0.98 ± 0.018	1.2 ± 0.015	0.21 ± 0.035	0.024 ± 0.0027	0.0014 ± 0.00072	0.11 ± 0.023	0.0067 ± 0.0036
	Aged 7	0.99 ± 0.26	1.5 ± 0.29	0.40 ± 0.079	0.02 ± 0.0041	0.016 ± 0.0033	0.049 ± 0.0040	0.039 ± 0.0035

[a]Uncertainty associated with each ratio is calculated based on the square root of the individual uncertainties multiplied by the ratio (Bevington, 1969).
[b]OM (organic mass) is calculated by subtracting major ions (i.e., sum of NH_4^+, NO_3^-, and $SO_4^=$), crustal components (2.2Al + 2.49 Si + 1.63 Ca + 1.94 Ti + 2.42 Fe) and elemental carbon from $PM_{2.5}$ mass.
[c]WSOC: water-soluble organic carbon
[d]Levoglucosan/2.25 represents carbon content in levoglucosan, based on the chemical composition $C_6H_{10}O_5$.
[e]Oxalate/3.75 represents carbon content in oxalate based on the chemical composition $C_2H_2O_4^=$.

https://doi.org/10.5194/amt-2019-198
Preprint. Discussion started: 29 May 2019

Atmospheric Measurement Techniques Discussions

(a) Upstream Filter Packs[a,b]

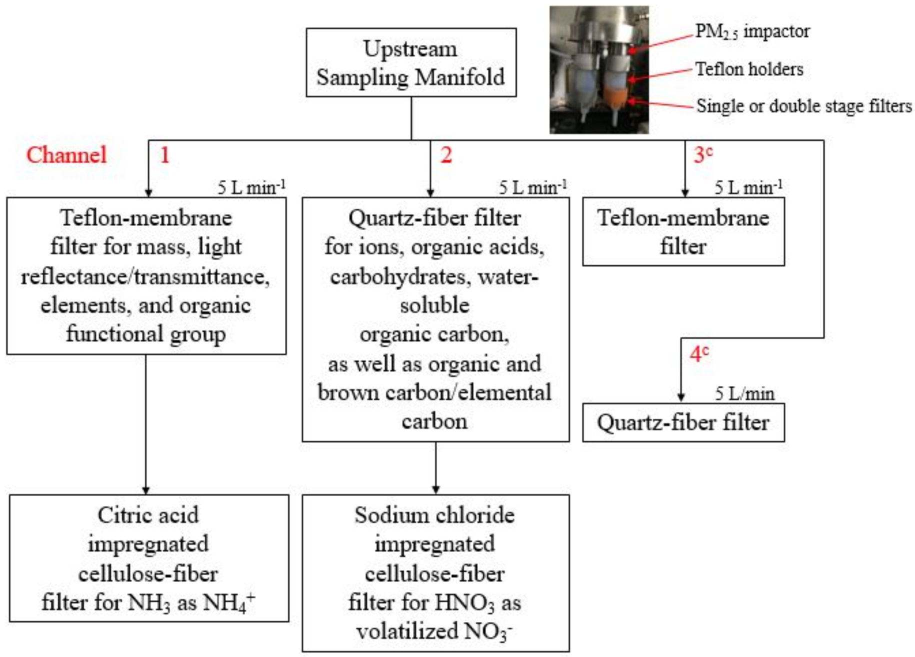

(b) Downstream Filter Packs[a,b]

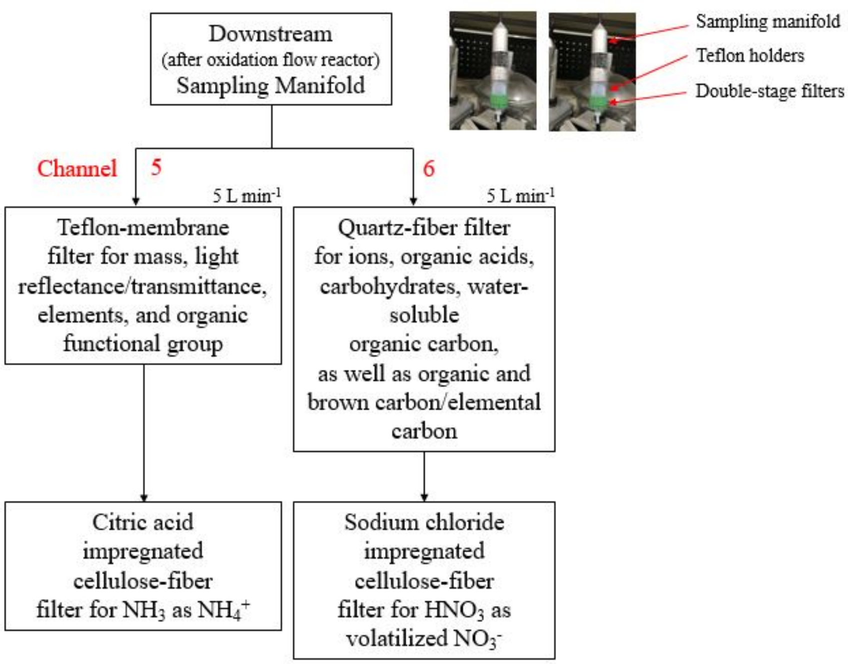

https://doi.org/10.5194/amt-2019-198
Preprint. Discussion started: 29 May 2019

[a]The filter types are: 1) Teflon-membrane filter (Teflo©, 2 µm pore size, R2PJ047, Pall Life Sciences, Port Washington, NY, USA); 2) quartz-fiber filters (Tissuquartz, 2500 QAT-UP, Pall Life Sciences); and 3) citric acid and sodium chloride impregnated cellulose-fiber filters (31ET, Whatman Labware Products, St. Louis, MO, USA).

[b]Analyses include: 1) mass by gravimetry (Model XP6 microbalance, Mettler-Toledo, Columbus, OH, USA); 2) light reflectance/transmittance by UV/Vis spectrometry (Lambda35, Perkin Elmer, Waltham, MA, USA); 3) multiple elements by energy-dispersive x-ray fluorescence (XRF) (Epsilon 5 PANalytical, Westborough, MA, USA); 4) four anions (chloride [Cl^-], nitrite [NO_2^-], nitrate [NO_3^-], and sulfate [$SO_4^{=}$]); three cations (water-soluble sodium [Na^+], potassium [K^+], and ammonium [NH_4^+]); and ten organic acids (i.e., formic acid/formate, acetic acid/acetate, lactic acid/lactate, methanesulfonic acid/methanesulfanate, oxalic acid/oxalate, propionate, succinic acid/succinate, maleic acid/maleate, malonic acid/malonate, and glutaric acid/glutarate) by ion chromatography (IC) with conductivity detector (Dionex Model ICS-5000+, Thermo Scientific, Waltham, MA, USA); 5) 17 carbohydrates (i.e., levoglucosan, mannosan, galactosan, glycerol, 2-methylerythritol, arabitol, mannitol, xylitol, erythritol, adonitol, inositol, glucose, galactose, arabinose, fructose, sucrose, and trehalose) by IC with pulsed amperometric detector (Dionex Model ICS3000, Thermo Scientific, Waltham, MA, USA); 6) water-soluble organic carbon (WSOC) by total organic carbon analyzer with non-dispersive infrared (NDIR) detector (Shimadzu Corporation, Kyoto, Japan); 7) organic functional groups by Fourier-Transform Infrared (FTIR) spectroscopy (VERTEX 70, Bruker, Billerica, MA, USA); and 8) organic, elemental, and brown carbon (OC, EC, and BrC) by multiwavelength thermal/optical carbon analyzer (DRI Model 2015, Magee Scientific, Berkeley, CA, USA).

[c]Teflon-membrane filter samples from Channel 3 are to be analyzed for additional organic nitrogen speciation using Fourier transform-ion cyclotron resonance mass spectrometry (FT-ICR-MS) at the Michigan Technological University. Quartz-fiber filter samples from Channel 4 are to be analyzed for polar and non-polar organics at the Hong Kong Premium Services and Research Laboratory.

Figure 1. Filter pack sampling configurations for upstream and downstream channels of the oxidation flow reactor.

https://doi.org/10.5194/amt-2019-198
Preprint. Discussion started: 29 May 2019

Atmospheric Measurement Techniques
Discussions

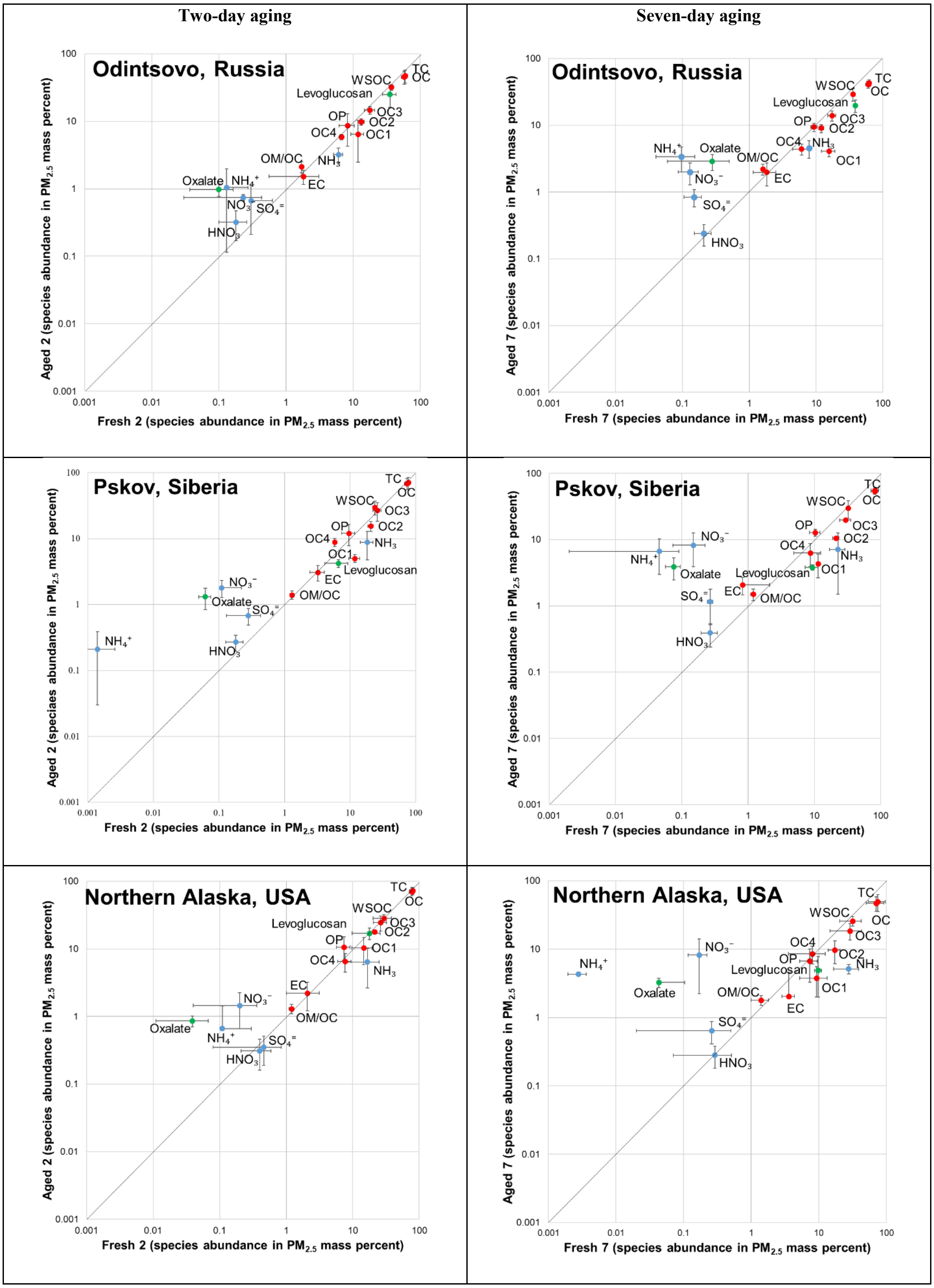

https://doi.org/10.5194/amt-2019-198
Preprint. Discussion started: 29 May 2019

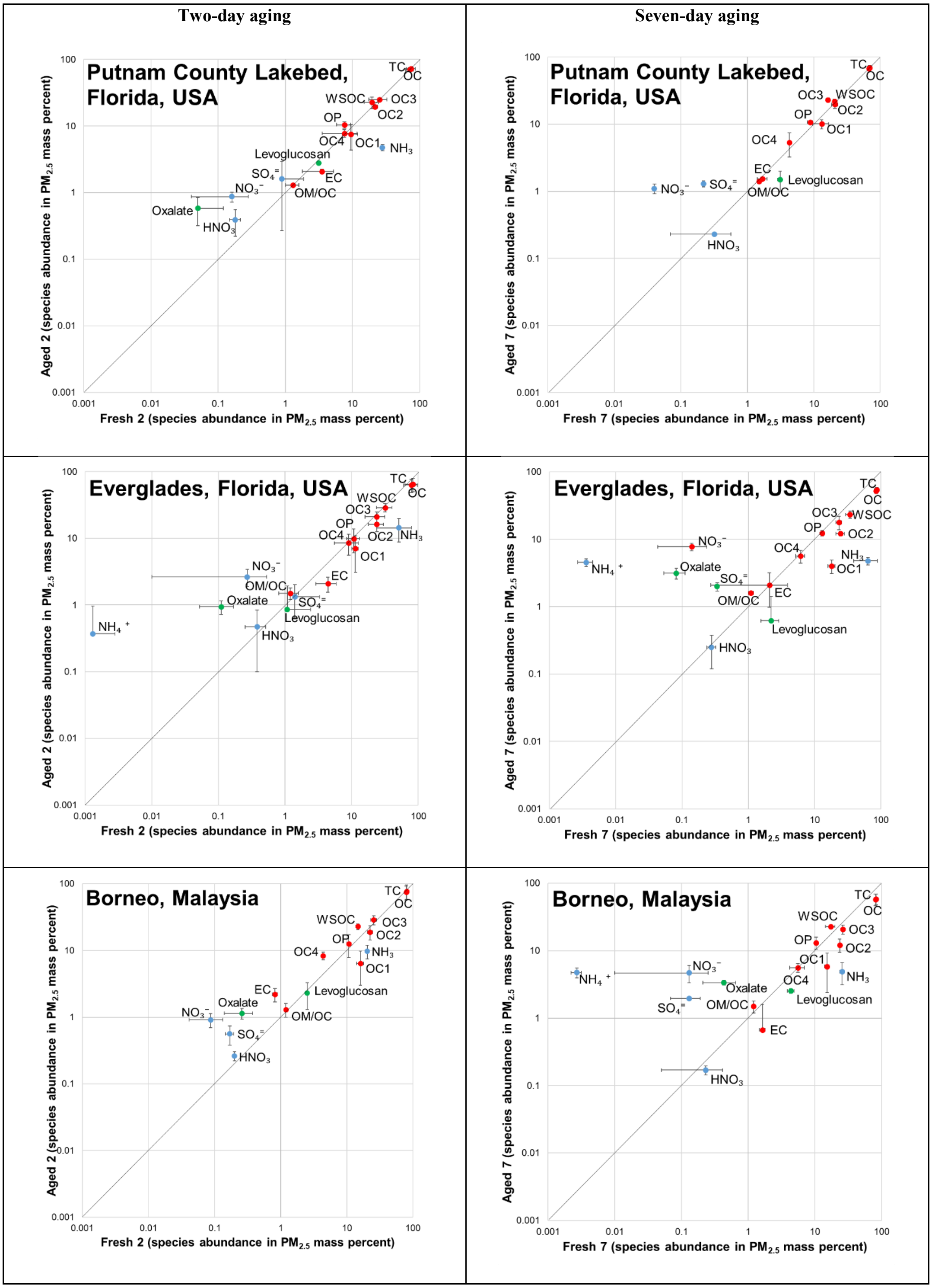

https://doi.org/10.5194/amt-2019-198
Preprint. Discussion started: 29 May 2019

Figure 2. Comparison between fresh and aged profile chemical abundances for each of the six types of peat with 2- and 7-day aging times. Standard deviations associated with averages in x and y axes are also shown.

https://doi.org/10.5194/amt-2019-198
Preprint. Discussion started: 29 May 2019

Atmospheric Measurement Techniques Discussions

756

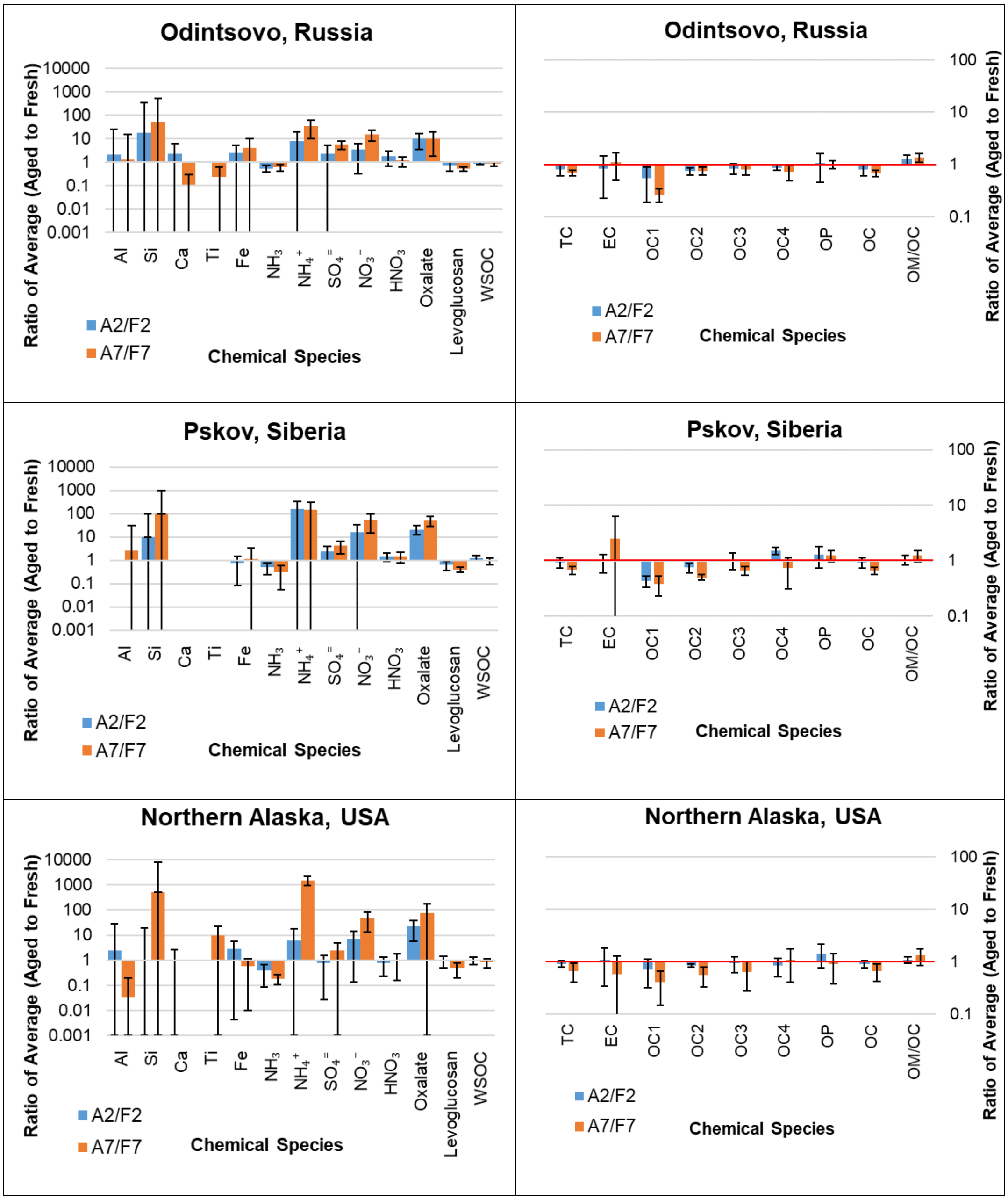

757

758

https://doi.org/10.5194/amt-2019-198
Preprint. Discussion started: 29 May 2019

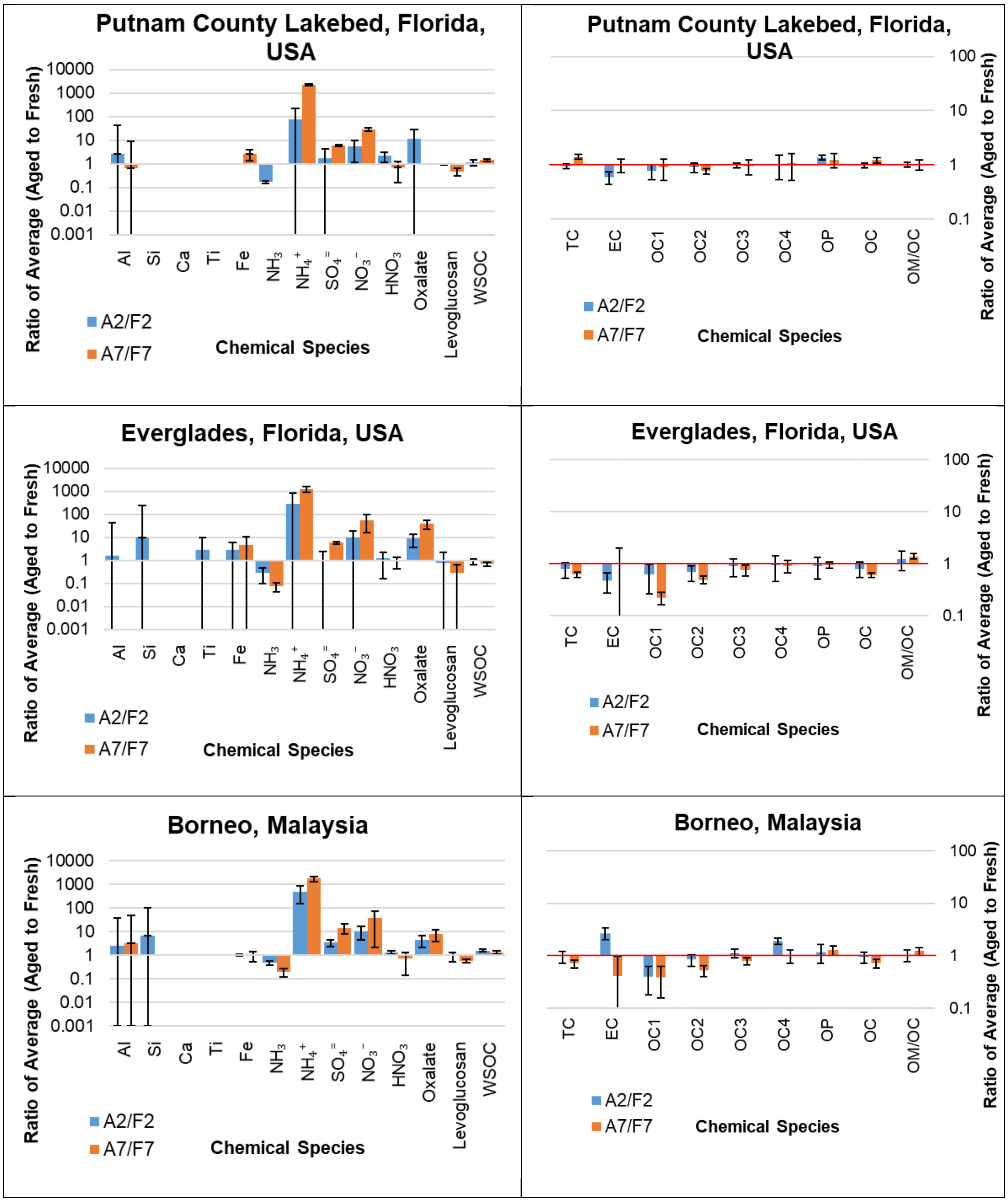

759 Figure 3. Ratios of average Aged (A) to Fresh (F) chemical species for 2-days (A2/F2) and 7-days
760 (A7/F7) of atmospheric aging of six types of peats. Vertical bars represent the standard deviations
761 associated with each ratio. Note that different scales were used in the two Y axes, with 0.001 to
762 10,000 on the left axis and 0.1 to 100 on the right axis (species abbreviations are shown in Fig. 1;
763 OM is organic mass).
764

https://doi.org/10.5194/amt-2019-198
Preprint. Discussion started: 29 May 2019

Atmospheric Measurement Techniques Discussions

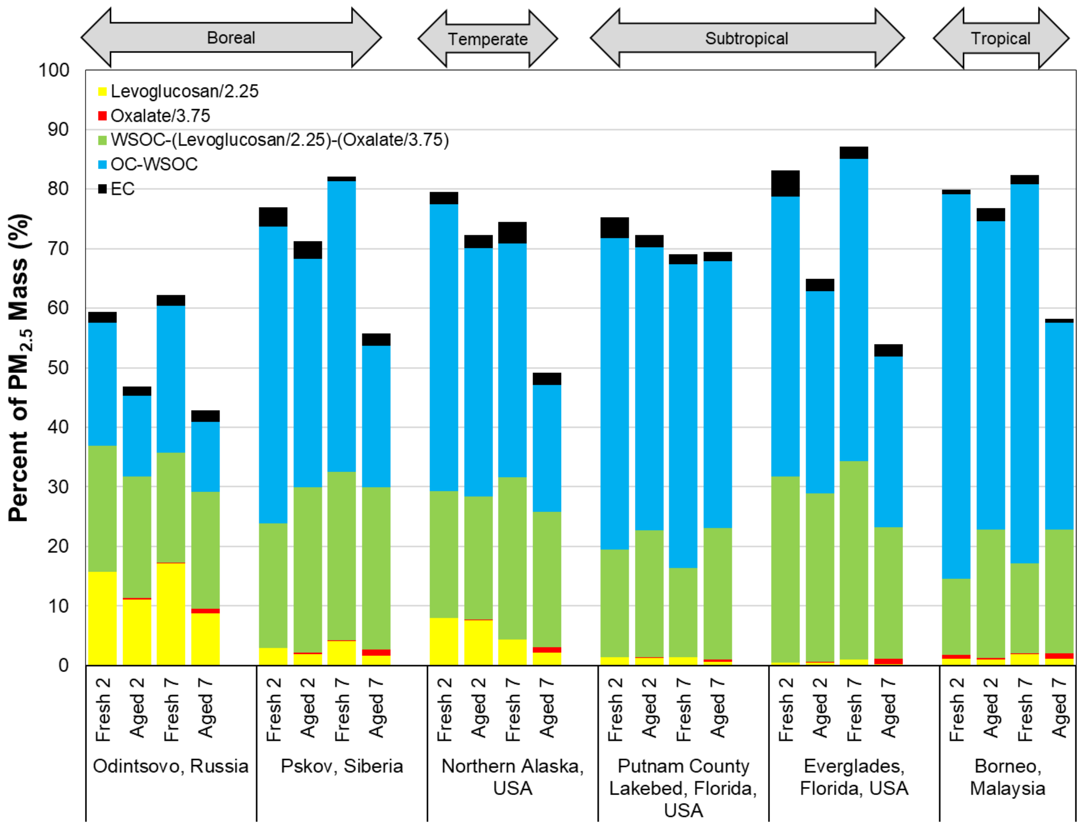

Figure 4. Abundances of fresh and aged carbon-containing components in $PM_{2.5}$ (levoglucosan [$C_6H_{10}O_5$] is divided by 2.25 and oxalate [$C_2H_2O_4^{=}$] is divided by 3.75 to obtain the carbon content. These levels are subtracted from the water-soluble organic carbon [WSOC] to obtain the remainder, and WSOC is subtracted from organic carbon [OC] to obtain non-soluble carbon. Elemental carbon [EC] is unaltered).

https://doi.org/10.5194/amt-2019-198
Preprint. Discussion started: 29 May 2019

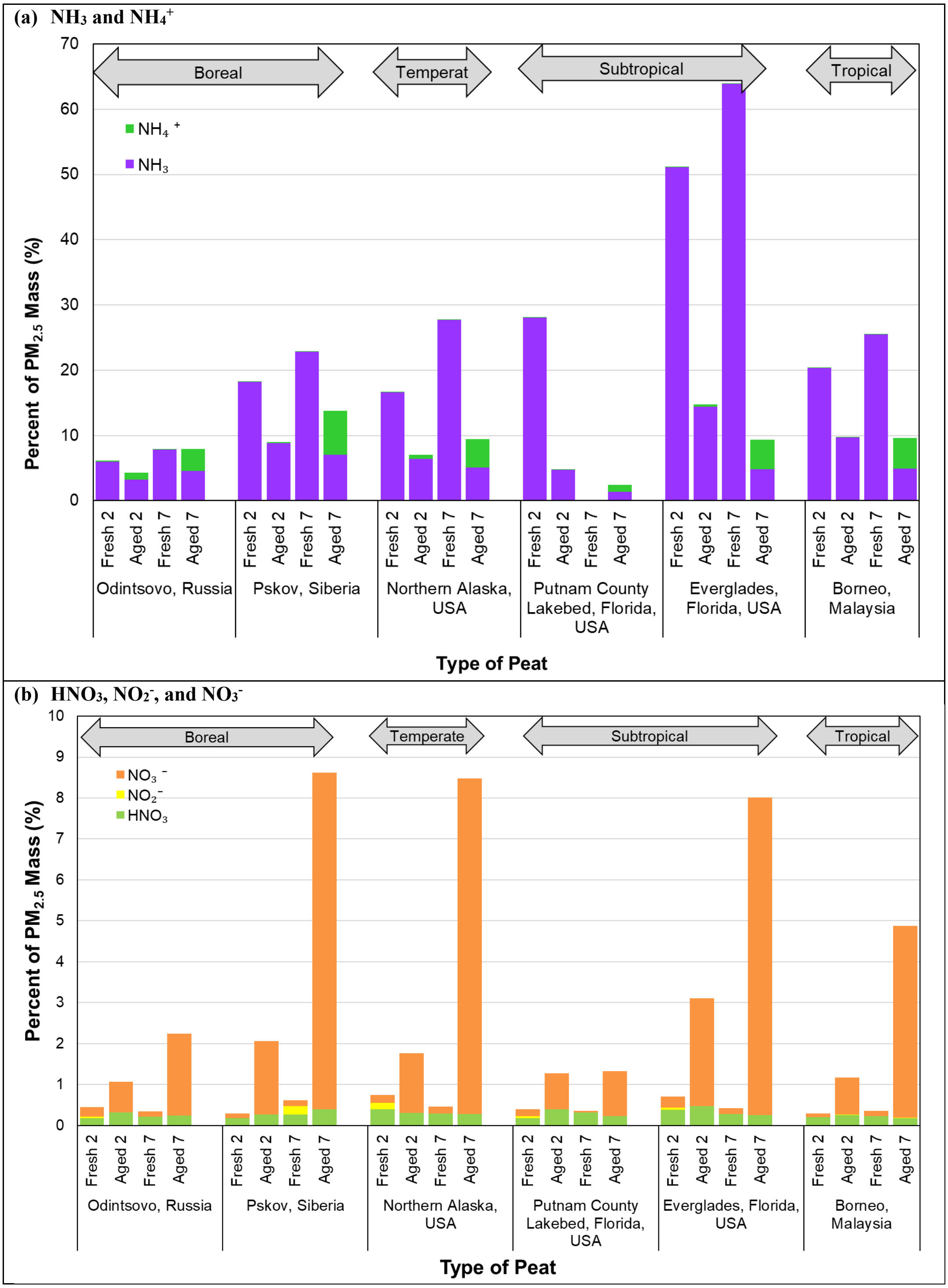

https://doi.org/10.5194/amt-2019-198
Preprint. Discussion started: 29 May 2019

Figure 5. Comparison of nitrogen species for: a) NH_3 and NH_4^+; and b) HNO_3, NO_2^-, and NO_3^- between fresh and aged profiles for six types of peats.

Atmospheric Measurement Techniques
Discussions

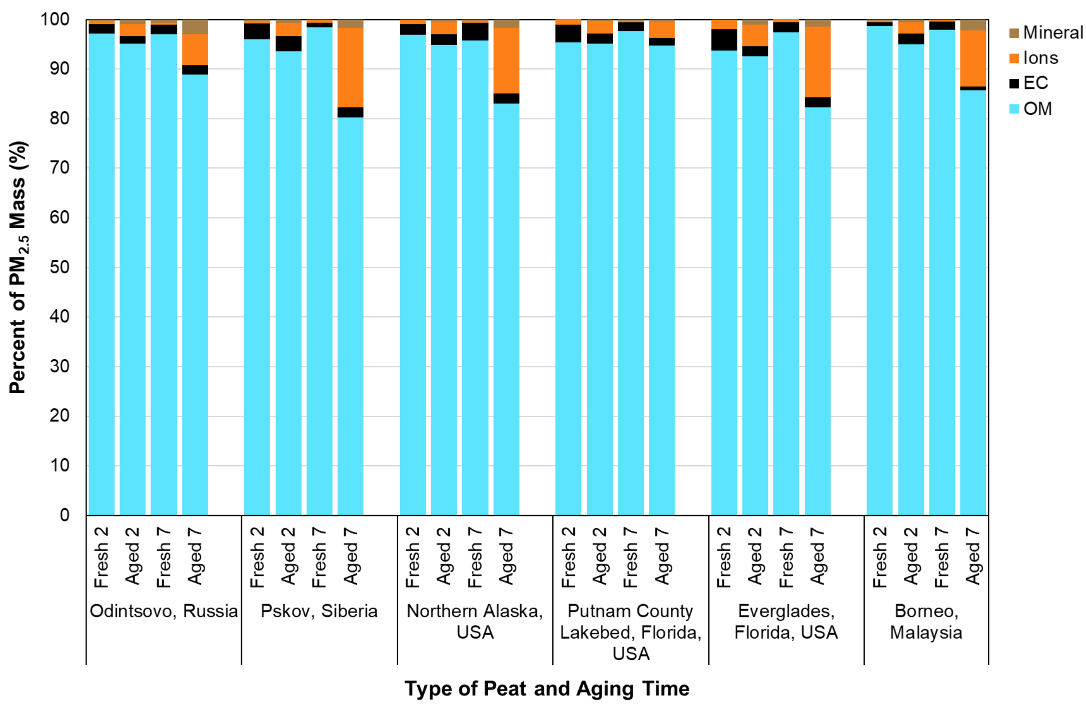

Figure 6. Reconstruction of $PM_{2.5}$ mass with organic matter (OM, see Table 3 for OM/OC ratios), elemental carbon (EC), major ions (i.e., sum of NH_4^+, NO_3^-, and $SO_4^=$), and mineral component (=2.2 Al + 2.49 Si + 1.63 Ca + 1.94 Ti + 2.42 Fe) for six types of peat between fresh and aged profiles.